NOAA Technical Memorandum ERL PMEL-56

TIDES AND TIDAL CURRENTS OF THE INLAND WATERS OF WESTERN WASHINGTON

Harold O. Mofjeld

Lawrence H. Larsen

School of Oceanography
University of Washington
Seattle, Washington

Pacific Marine Environmental Laboratory
Seattle, Washington
June 1984

UNITED STATES DEPARTMENT OF COMMERCE

Malcolm Baldrige, Secretary

NATIONAL OCEANIC AND ATMOSPHERIC ADMINISTRATION

John V. Byrne, Administrator

Environmental Research Laboratories

Vernon E. Derr Director

NOTICE

Mention of a commercial company or product does not constitute an endorsement by NOAA Environmental Research Laboratories. Use for publicity or advertising purposes of information from this publication concerning proprietary products or the tests of such products is not authorized.

CONTENTS

Figures

Tables

Glossary

amplitude	maximum of a tidal constituent's tide or tidal current
apogee	condition when the moon is at its farthest distance from the earth
apogean range	semidiurnal range at apogee
declination	angular distance north or south of the equator
diurnal	occuring once a day
diurnal age	time elapsed from maximum diurnal forcing until the maximum diurnal tides
diurnal inequality	difference in successive low water - high water ranges on a given day
ebb	motion toward the entrance to the ocean
epoch	period of repetition (18.6 years) for long-term variations in the lunar tides
equilibrium tide	hypothetical tide that would occur if the ocean responded instantly to tidal forcing
equinox	condition when the sun is directly above the equator
flood	motion away from the entrance to the ocean
fortnightly	occuring every two weeks
Greenwich phase lag	time (in units of degrees) elapsed from Greenwich transit of a tidal constituent until its high water (or maximum flood current)
Greenwich transit	passage over the Greenwich meridian and phase reference for tidal constituents
harmonic analysis	method for estimating harmonic constants from time-series based on the sinusoidal nature of the tidal constituents
high water	temporary maximum in height of the sea surface
internal seiche	standing internal wave
internal wave	wave propagating in the interior of the water driven by the interior mass distribution
isobath	line of constant water depth
K_1	principal diurnal declinational (luni-solar) tide
low water	temporary minimum in the height of the sea surface

lunitidal interval	time elapsed from Greenwich transit until high water of the M_2 tidal constituent
M_2	principal semidiurnal lunar constituent
major amplitude	highest strength of a tidal constituent's current
mean high water	average of the high waters (usually two-occurring each day) over a 19 year period
mean higher high water	averages of the highest waters occurring each day over a 19 year period
mean lower low water	average of the lowest waters occurring each day over a 19 year period
mean range	average vertical displacement between low and high water
mean sea level	average height of sea level over a 19 year period
minor amplitude	minimum strength of a tidal constituent's current
mixed-diurnal	occurring primarily once a day but with significant semidiurnal variations, especially when the moon is near the equator
mixed-semidiurnal	occurring primarily twice a day with 2 distinct differences between successive high or low waters
N_2	larger semidiurnal lunar elliptic constituent
neap	occurring during quarter moon (moon and sun in quadrature)
node	location where the tide of a tidal constituent has zero (or very small) amplitude
O_1	principal diurnal lunar constituent
parallax age	time elapsed from lunar perigee until the maximum semidiurnal lunar tide
perigee	condition when the moon is at its closest approach to the earth
perigean range	semidiurnal range at perigee
phase age	time elapsed from full (or new) moon until the maximum semidiurnal tides
precession	slow movement of the moon's orbital ellipse causing long-term (18.6 year period) variations in the lunar tides

range	vertical displacement between sucessive low and high waters
S_2	principal semidiurnal solar constituent
semidiurnal	occurring twice a day
sequence of tide	phase relationship between M_2, K_1 and O_1 responsible for the shape of tidal time-series when the moon is away from the equator
solstice	condition when the sun is farthest from the equator (largest declination)
spring	semidiurnal tides or tidal currents at full or new moon
spring-neap	occurring as the moon and sun go in and out of alignment
standing wave	a non-propagating pattern formed by incident and reflected waves
tide	vertical displacement of the sea surface caused by the gravitational attraction of the moon and sun
tidal constituent	component of the tidal motion occurring at a given (constant) frequency
tidal current	rate of horizontal tidal motion
tidal curve	time-series of the tide
tidal datum plane	horizontal surface defined by an average tidal height such as mean lower low water
tidal eddy	small, recirculating motion generated by tidal currents
tidal ellipse	ellipse formed by the tips of the tidal current arrows during one cycle of a tidal constituent
tidal exchange	water transferred by tidal motions back and forth between separate regions
tidal excursion	horizontal displacement caused by the tidal currents
tidal front	sharp horizontal change in the tidal currents or water properties caused by tidal motions
tidal intrusion	water brought into a region by tidal motions
tidal prism	change in water volume of a region occurring within a tidal cycle
tidal transport	volume of water moved past a cross-section by tidal motions

tropic	condition when the moon is farthest from the equator (maximum declination)
tropic-equatorial	occurring as the lunar declination varies through its cycle
type of tide	ratio of the diurnal (K_1+O_1) tidal amplitudes to the semidiurnal tidal amplitudes (M_2+S_2) indicating the relative importance of the diurnal and semidiurnal tides (or tidal currents)

Tides and Tidal Currents of the Inland Waters of Western Washington[1]

Harold O. Mofjeld and Lawrence H. Larsen

ABSTRACT. The tides enter the inland waters of Western Washington from the Pacific Ocean. They form a pattern of nearly standing waves with large areas of relatively constant amplitude and phase separated by channels where both change rapidly. The tides are either mixed-semidiurnal or mixed-diurnal. Usually the tides have nearly equal high waters with large differences in the low waters. The diurnal range decreases from 2.4 m at the western end (Neah Bay) of the Strait of Juan de Fuca to a minimum of 1.9 m at the southern end of Vancouver Island (Victoria, British Columbia) and then increases to 4.4 m at the southern end of Puget Sound (Olympia). There is an increase in phase lag away from the ocean due to tidal dissipation. This dissipation is large compared with inland waters with smooth bottom topography and is concentrated in the rugged channels such as Admiralty Inlet and Haro Strait with strong tidal currents.

The tidal currents often exceed 1 m/s in many channels and the Strait of Juan de Fuca. Weaker currents occur in the main basins and side-embayments. Strong vertical shear occurs over sills but the tidal currents are relatively independent of depth in the deeper reaches. The tidal currents are rectilinear and flow parallel to the local channel or shoreline except at the intersection of several channels where broad tidal ellipses can occur. In Admiralty Inlet there are major diurnal inequalities in both the flood and ebb currents while in The Narrows the ebb currents are nearly equal in strength. The tidal prism of Puget Sound amounts to 4.8% of its total volume. Associated with the tidal currents are numerous eddies, fronts and internal waves.

---

[1] Contribution number 687 from the NOAA/ERL Pacific Marine Environmental Laboratory, 7600 Sand Point Way NE, Seattle, Washington 98115.

1. Introduction

The tidal motions of the inland waters of Western Washington have been under study for many years. The permanent tide gage at Seattle (Fig. 1) was installed in 1899, and the first description of the tides of the region was published by Harris in 1904. The first current survey (Cox et al., 1981) in Puget Sound was made in 1908-1909. Since then, several tide and current surveys of the region have been carried out by the United States Coast and Geodetic Survey and its successor, the National Ocean Survey, to aid navigation and to define shorelines and datum planes. The National Ocean Survey uses these observations for many of its publications on tides and tidal currents of the region: tide and tidal current tables, tidal current and nautical charts and the United States Coast Pilot.

In the 1970's the emphasis of the field work and modelling shifted in response to environmental issues. Extensive surveys of tides and currents in the Straits of Juan de Fuca-Georgia and Puget Sound were made by the National Ocean Survey and the Pacific Marine Environmental Laboratory, in cooperation with the government of Canada. Results for the Straits have been published by Parker (1977a), Cannon et al. (1978) and Holbrook et al. (1980). Although the results from Puget Sound have not been published, they have been made available to the authors by B. Parker (National Ocean Survey) and G. Cannon (Pacific Marine Environmental Laboratory) for use in this memorandum.

A comparison of simple theories (Harris 1904, Redfield 1950, Rattray in Department of Oceanography, University of Washington 1954, Parker 1977b) with observations shows that the tides in the region are formed by long waves which propagate into the system from the Pacific Ocean and reflect to form patterns of nearly standing waves. The waves enter mainly through the

Strait of Juan de Fuca with a small contribution through Johnstone Strait at the northern end of the Strait of Georgia. Partial reflection occurs at several intermediate locations along the axes of the system (Rattray, in Department of Oceanography, University of Washington 1954, Parker 1977b, 1980). The tidal motions of the region are subject to unusually strong dissipation (Redfield 1950) which appears to be concentrated in channels connecting major basins (Rattray, in Department of Oceanography, University of Washington 1954, Crean 1969) or near the heads of the system (Parker 1977b, 1980). Over the broad reaches of the Strait of Juan de Fuca, the earth's rotation causes significant variations in the tides across the strait (Harris 1904, Parker 1977b). Non-linear effects are also important (Crean 1969).

The tidal currents are generally aligned with the direction of the local channel. Their phases relative to the tides' are consistent with standing waves subject to friction (Bauer 1928). The tidal currents have a great deal of fine structure that requires detailed modelling to simulate. Numerous eddies, internal waves and fronts are generated by the tidal currents. Vertically-averaged models (Crean 1978, Jamart and Winter 1978) have been developed to study these features in limited locations within the region. There are also multi-level models (Crean, private communication) under development to study the vertical structure of the tidal currents.

In this memorandum we shall summarize what is known about the tides and tidal currents of the region as seen from observations and numerical models. The region of interest includes the Strait of Juan de Fuca and the southern Strait of Georgia as well as Puget Sound. This is because the tidal motions in the straits drive those in Puget Sound to form a unified, co-oscillating system. There are also many similarities in the tidal dynamics of Puget Sound and the straits, and the insights gained from studying the tidal

motions in the straits are useful in understanding those in Puget Sound. Enough is known about the tides and tidal currents of the combined system to provide a general description of the tidal motions and to identify many of the processes that control these motions. However, the region is so complex that the details of the tidal distributions and the tidal dynamics remain to be worked out.

2. Tides

2.1 Patterns of Tidal Curves

Both the diurnal and semidiurnal tides are important in the region (Fig. 1). Typical tidal curves (Fig. 2) are either mixed-diurnal or mixed-semidiurnal in type. Tidal ranges (Table 1) are several meters with the maximum diurnal range (4.4 m) in the southern-most reaches of Puget Sound (Olympia). The phase relationship between the diurnal and semidiurnal tides (sequence of tide around 180°) causes nearly equal high waters but produces a large inequality in the low waters, except during the short time when the moon is near the equator (Fig. 2). The influence of the diurnal tide is particularly strong in the eastern Strait of Juan de Fuca (Victoria) where the semidiurnal (mean) range is a minimum.

The fortnightly variations in range are due primarily to the tropic-equatorial modulations in the diurnal tides. This is because the diurnal tides are relatively strong in the region and because the semidiurnal solar tide S_2 is relatively small (Tables 2 and 3), producing only a modest spring-neap modulation in the semidiurnal tides. Figure (2) shows that the monthly modulations in the semidiurnal tide are comparable with the

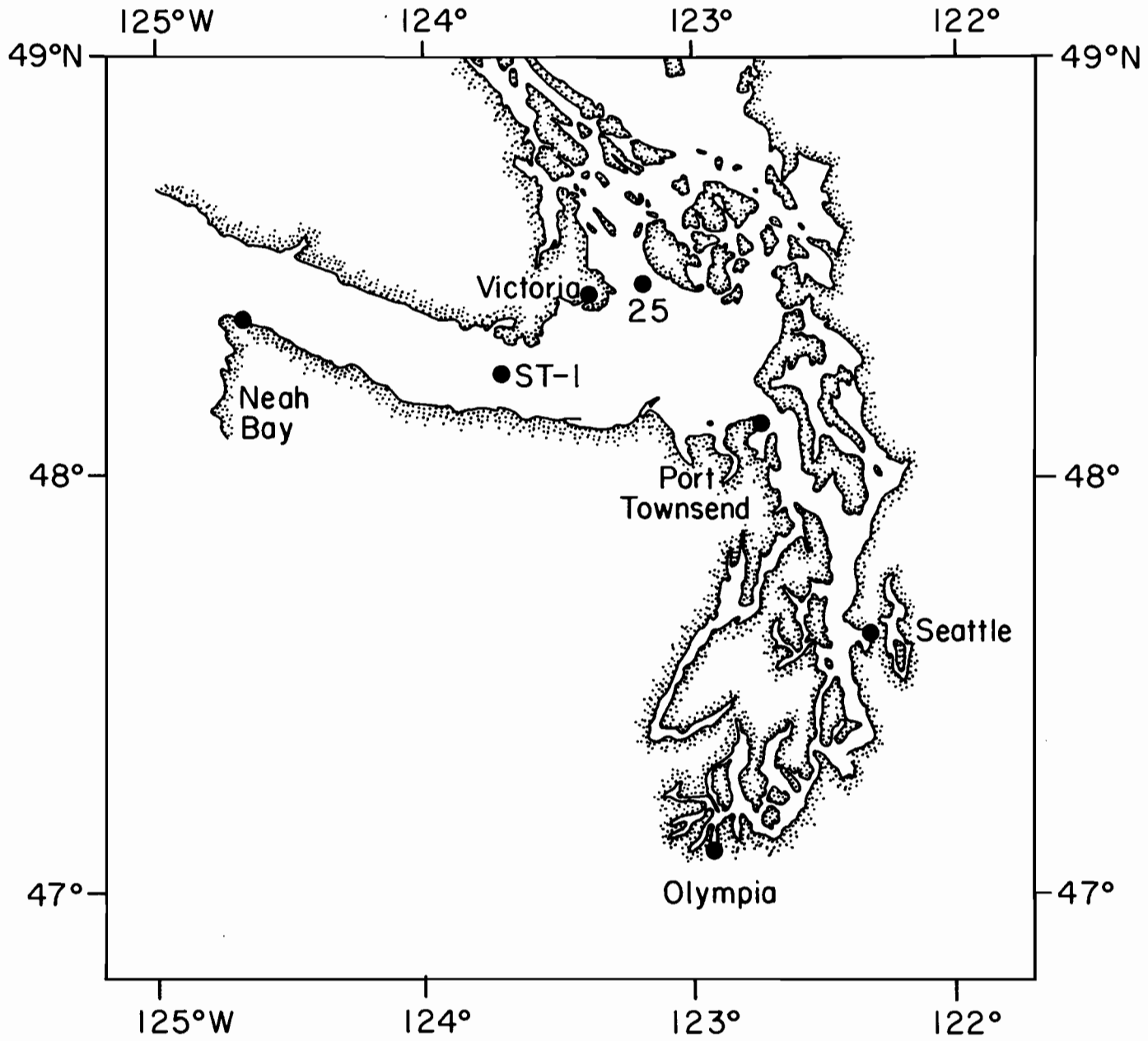

Figure 1. Chart of Puget Sound and the southern Straits of Juan de Fuca-Georgia showing the locations of representative tide stations (Tables 1-3) and representative tidal current stations ST-1 and 25 (Tables 4 and 5) for the Strait of Juan de Fuca.

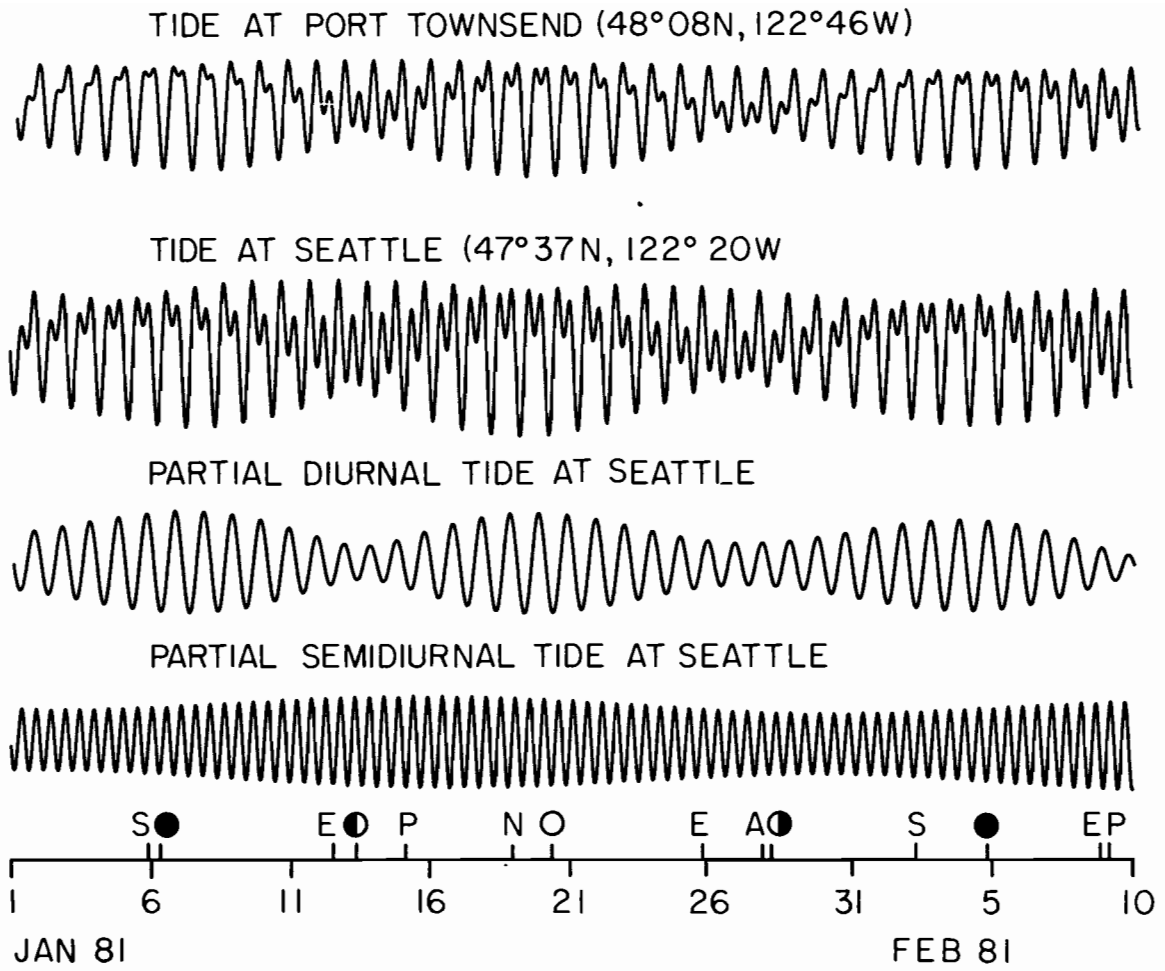

Figure 2. Predicted tides at Port Townsend and Seattle (Fig. 1) based on the eight tidal constituents in Table 2. Also shown are partial diurnal and semidiurnal tides at Seattle. The symbols along the time axis refer to positions of the moon: S = extreme southern declination, ● = new moon, E = moon on the equator, ◐ = first quarter, P = moon at perigee, N = extreme northern declination, ○ = full moon, A = moon at apogee, ◑ = last quarter.

Table 1. General tidal characteristics[1] at selected tide stations in the Puget Sound Region (Fig. 1) computed from the harmonic constants in Table 2.

STATION	Neah Bay	Victoria	Port Townsend	Seattle	Olympia
Type of tide $\frac{K_1+O_1}{M_2+S_2}$	0.79	2.10	1.44	0.97	0.75
Sequence of tide M_2^o-K_1^o-O_1^o	126	159	190	198	199
Range (m)					
Mean[2]	1.7	(0.8)	1.6	2.3	3.2
Diurnal[2]	2.4	1.9	2.6	3.4	4.4
Spring 2.1(M_2+S_2)	2.1	1.0	1.8	2.8	3.8
Neap 2.1(M_2-S_2)	1.2	0.6	1.1	1.7	2.3
Perigean 2.2(M_2+N_2)	2.1	1.0	1.8	2.8	3.8
Apogean 2.2 M_2-1.7 N_2	1.4	0.7	1.2	2.0	2.7
Interval (h)					
Lunitidal M_2^o/28.98	8.5	10.9	12.1	12.8	13.5
Phase age 0.984(S_2^o-M_2^o)	27	17	24	27	33
Parallax age 1.837(M_2^o-N_2^o)	42	57	55	57	50
Diurnal age 0.911(K_1^o-O_1^o)	15	20	19	20	21

[1] formulas derived by Zetler (1959).
[2] values taken from tide tables (National Ocean Survey 1979)

Table 2. Tidal harmonic constants for selected tide stations in the Strait of Juan de Fuca and Puget Sound. Phase lags G° are relative to Greenwich transit. Values from various sources published by the United States Coast and Geodetic Survey and the National Ocean Survey.

	Constituent	Period	Station: Neah Bay 48°22'N 124°37'W		Victoria 48°26'N 123°37'W		Port Townsend 48°37'N 122°46'W		Seattle 47°37'N 122°20'W		Olympia 47°03'N 122°54'W	
		(days)	H(cm)	G°	H(cm)	G°	H(cm)	G°	H(cm)	G°	H(cm)	G°
Long Period	Sa	365.24	13.6	314	-	-	8	288	7	289	-	-
	Ssa	182.62	2.8	272	-	-	4	225	3	215	-	-
		(hours)										
Diurnal	Q_1	26.87	5.5	222	6.4	239	7.3	242	7.5	250	7.9	259
	O_1	25.82	30.7	232	36.3	248	44.3	250	45.6	256	47.6	264
	P_1	24.07	15.3	245	19.2	267	24.2	270	25.2	275	25.5	286
	K_1	23.93	49.2	248	63.1	270	76.1	271	82.5	278	87.9	287
Semidiurnal	N_2	12.66	16.5	223	8.8	286	14.2	321	20.9	341	27.5	3
	M_2	12.42	78.0	246	36.9	317	67.0	351	106.6	12	145.3	30
	S_2	12.00	22.6	273	10.4	334	16.4	15	26.0	39	34.4	64
	K_2	11.97	5.9	266	1.8	341	4.7	18	7.7	38	10.4	57
Quarter Diurnal	M_4	6.21	1	61	-	-	4	61	2	195	6	288
Sixth Diurnal	M_6	4.14	-	-	-	-	1	249	1	302	3	140
Remarks			Least squares analysis of 2-year series		Mean of 15 harmonic analyses of 1-year series		Mean of 4 harmonic analyses of 1-year series		Mean of 5 harmonic analyses of 1-year series		Harmonic analysis of 1-year series	
			Sa and Ssa from long records of mean monthly sea level									

Table 3. Ratio of amplitude for the major tidal constituents for selected stations in the Strait of Juan de Fuca and Puget Sound computed from the harmonic constants in Table 2.

Tidal Constituents	Equilibrium	STATION				
		Neah Bay	Victoria	Port Townsend	Seattle	Olympia
Diurnal						
Q_1/O_1	0.19	0.18	0.18	0.16	0.16	0.17
O_1/K_1	0.71	0.62	0.58	0.58	0.55	0.54
P_1/K_1	0.33	0.31	0.30	0.32	0.31	0.29
Semidiurnal						
N_2/M_2	0.19	0.21	0.24	0.21	0.20	0.19
S_2/M_2	0.47	0.29	0.28	0.24	0.24	0.24
K_2/S_2	0.27	0.26	0.17	0.29	0.30	0.30

fortnightly modulations. This can also be seen from semidiurnal amplitudes (Tables 2 and 3): N_2 (associated with the monthly modulation) is nearly as large as S_2 (associated with the fortnightly modulation). Both semidiurnal modulations lag in time their equilibrium counterparts. For the fortnightly modulation of S_2 and M_2 the corresponding phase age (Table 1) increases from 23 hours at the entrance (Port Townsend) to Puget Sound to 33 hours at the southern end (Olympia). On the other hand, the parallax age associated with the monthly modulation (N_2 and M_2) does not show a trend; in Puget Sound, the average parallax age is 54 hours. The diurnal age (O_1 and K_1) is about 20 hours.

There is a seasonal relationship between spring and tropic tides. As discussed by Crean (1969), at the solstices (December and June) new and full moons occur at times of large lunar and solar declinations. The spring and tropic tides then coincide, giving rise to large tidal ranges and inequalities. At the equinoxes, new and full moons occur when the moon and sun are near the equator. Then, spring tides have small inequalities and neap tides have large inequalities. Because of the relationship between the phases of M_2, K_1, and O_1 in the region, the lowest tides occur at night during the winter and during the day in summer. The tides have variations through the year because earth's orbit around the sun is inclined (23.5°) relative to the equator and because the orbit is elliptical.

Over several years the lunar constituents vary periodically due to the 18.6-year precession of the moon's orbit. The harmonic constants (Table 2) are averages over the precessional period (19 years in practice). The major effect is due to the declination of the moon which varies from 18.3° to 28.6° and has a significant effect on the amplitudes of O_1 (~18%) and K_1 (~11%). The larger semidiurnal constituents M_2 and N_2 are much less affected (~4% each). It is over the precessional period that the United

States Coast and Geodetic Survey (Marmer, 1951) averages tidal heights to obtain the tidal datum planes. One of these, mean lower low water MLLW is the reference plane for nautical charts along the west coast of the United States. By direct averaging over three 19-year epochs (1899-1917), 1915-1933, 1930-1948) Marmer (1951) found for Seattle that relative to mean lower low water, the heights of the tidal datums mean higher high water and mean sea level were 3.192, 3.189, 3.199 m and 2.023, 2.018, 2.025 m, respectively. Discussions of seasonal and longer period variations and trends in sea level are given by Marmer (1951), Waldichuk (1964), and Hicks (1973).

2.2 Geographical Distributions of the Tides

The geographical distributions of the semidiurnal and diurnal tides can be represented by the largest constituent of each species since the ratios of constituents (Table 3) remain relatively constant over the region. Typical of the semidiurnal tides, the M_2 tide varies considerably within the region. Following the changes in M_2 phase lag from the entrance of the Strait of Juan de Fuca, the M_2 phase (Fig. 3) increases eastward through the western Strait of Juan de Fuca and more rapidly in the eastern Strait and the San Juan Archipelago. In the Strait of Georgia, the northward increase in M_2 phase is small particularly in the northern reaches. The total increase in M_2 phase through the Staits of Juan de Fuca - Georgia is about 148°. The M_2 amplitude (Fig. 4) decreases dramatically from the entrance to a minimum at the southern end of Vancouver Island. After increasing rapidly through the San Juan Archipelago, the M_2 amplitude increases more gradually in the southern Strait of Georgia and is nearly constant over the northern reaches of the system where the M_2 amplitude is slightly larger (1.3×) than its value at the entrance to the Strait of Juan de Fuca.

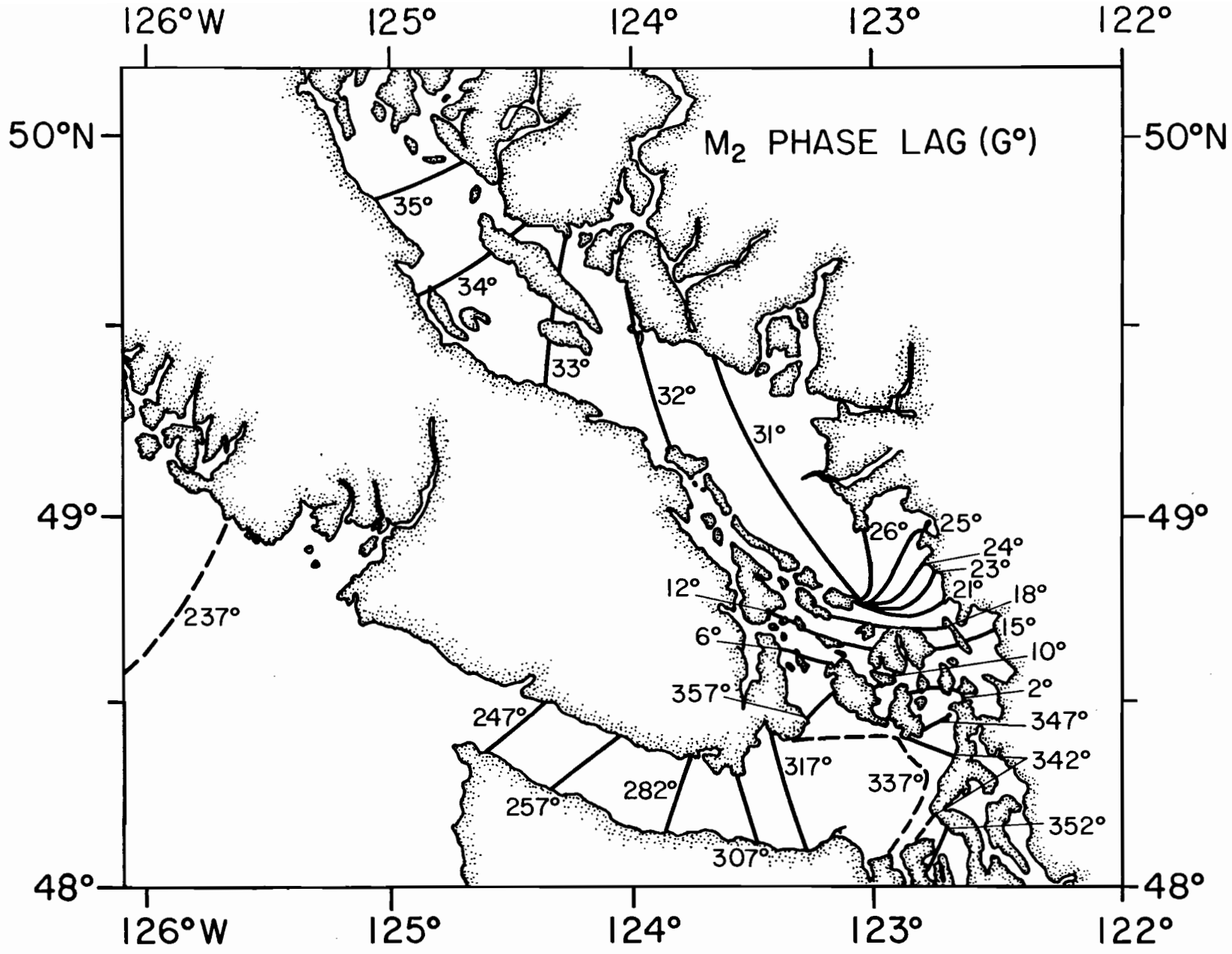

Figure 3. Empirical cophase lines of the M_2 tide in the Straits of Juan de Fuca-Georgia based on a dense net of coastal stations. Dashed lines indicate uncertainty in position. The numbers are phase lags in degrees since Greenwich transit. Modified from Parker (1977a).

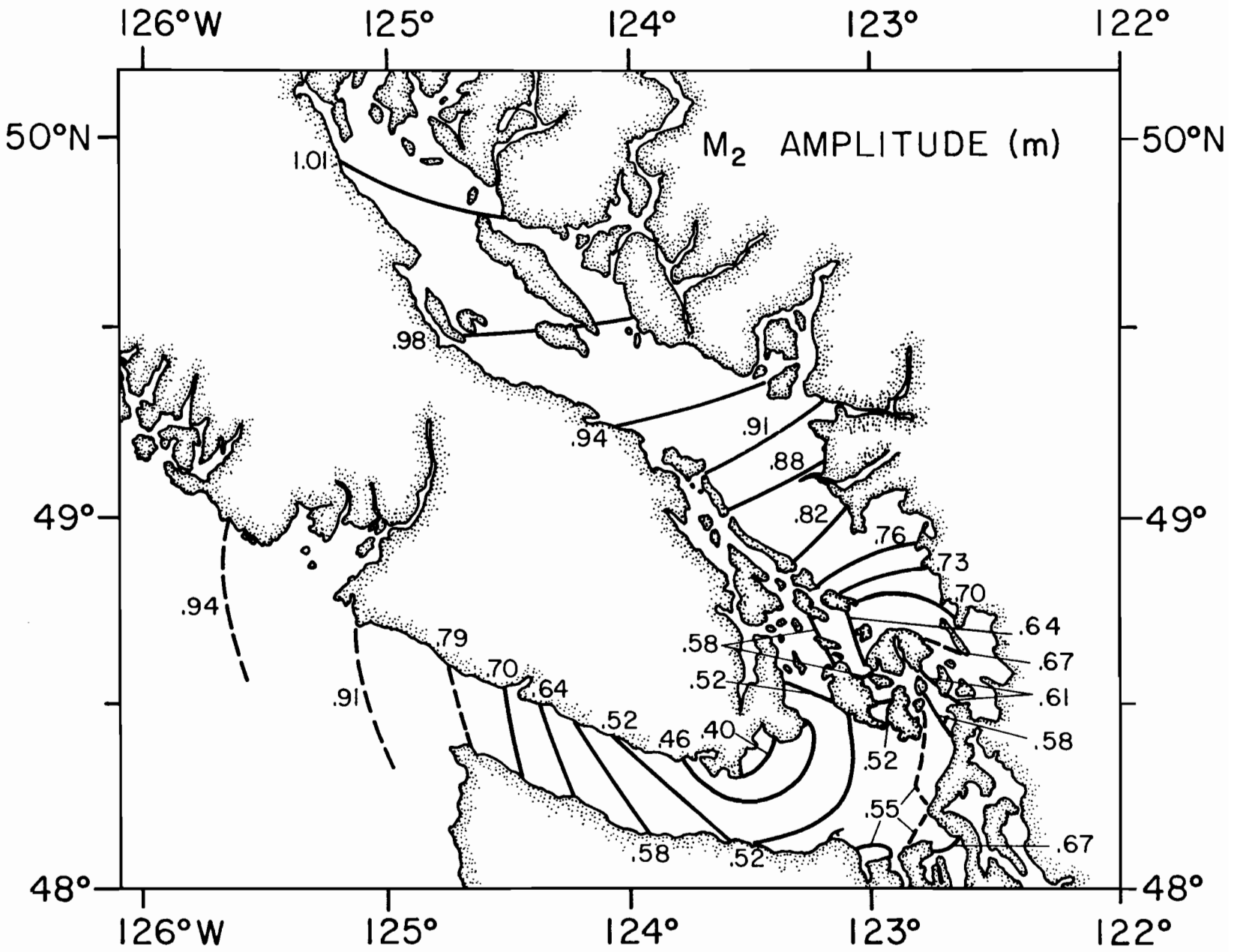

Figure 4. Empirical co-amplitude lines of the M_2 tide in the Straits of Juan de Fuca-Georgia based on a dense net of coastal stations. Dashed lines indicate uncertainty in position. The numbers are amplitudes in meters. Modified from Parker (1977a).

Like the other diurnal tides, the K_1 tide increases continuously in phase lag and amplitude through the system. In the Straits of Juan de Fuca - Georgia (Figs. 5 and 6) the largest increases in phase and amplitude occur in the western Strait of Juan de Fuca and through the San Juan Archipelago. The total changes in K_1 through the overall system are 39° in phase and a factor of 2.0 in amplitude. According to Redfield (1950) both the incident M_2 (4.83 hrs) and K_1 (4.92 hrs) waves take about 5 hours to propagate from Clayoquot on the Pacific Coast to Whaleton in northern Strait of Georgia. Each slows down on entering the Strait of Juan de Fuca, each proceeds at 18 m/s (35 knots) between Port Angeles and Point Atkinson, British Columbia, and then speeds up dramatically in upper Strait of Georgia. Redfield noted that relative to the K_1 wave the M_2 wave undergoes a delay of about ½ hour in the intermediate channels of the system.

In Puget Sound (Fig. 7 and 8) the M_2 phase and amplitude increase toward the heads of the system; they increase most rapidly through Admiralty Inlet and The Narrows and are relatively constant in the major basins. The total M_2 phase increase (Table 2) in Puget Sound is 39°. There are also large phase increases in the narrow channels connecting two small basins, Dyes Inlet and Oakland Bay, with the main system. Along the main axis of Puget Sound, the M_2 amplitude increases by a factor of 2.2 from the northern end of Admiralty Inlet (Port Townsend) to the southern end of the southern basin (Olympia). In Puget Sound (Table 2, Figs. 9 and 10) the total increase in K_1 phase (16°) and amplitude (1.2×) are relatively small.

Tidal Dynamics

There are a number of theoretical models which provide considerable insight into the tidal behavior of the region. While many of the details remain to be worked out, the important processes controlling the tides

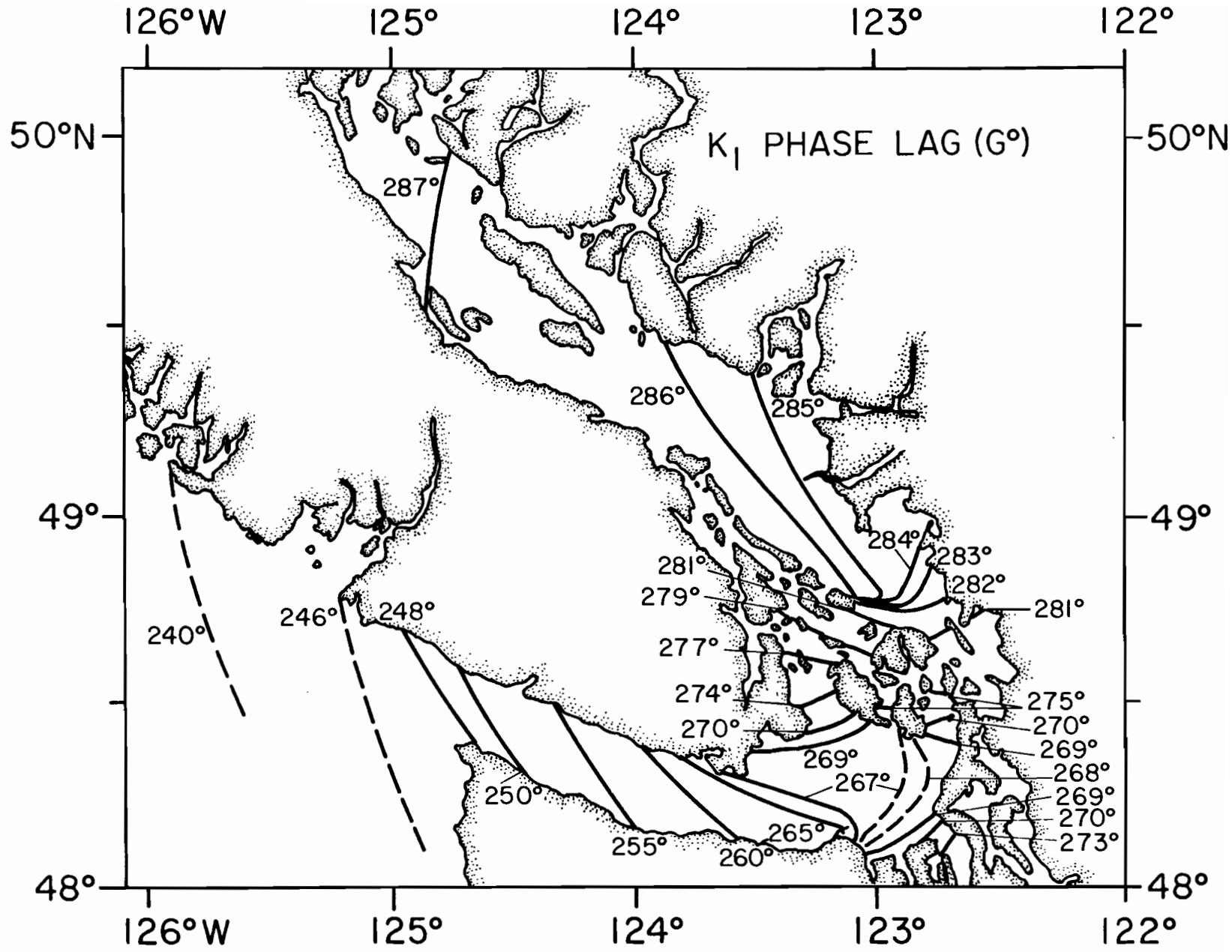

Figure 5. Empirical cophase lines of the K_1 tide in the Straits of Juan de Fuca-Georgia based on a dense net of coastal stations. Dashed lines indicate uncertainty in position. The numbers are phase lags in degrees since Greenwich transit. Modified from Parker (1977a).

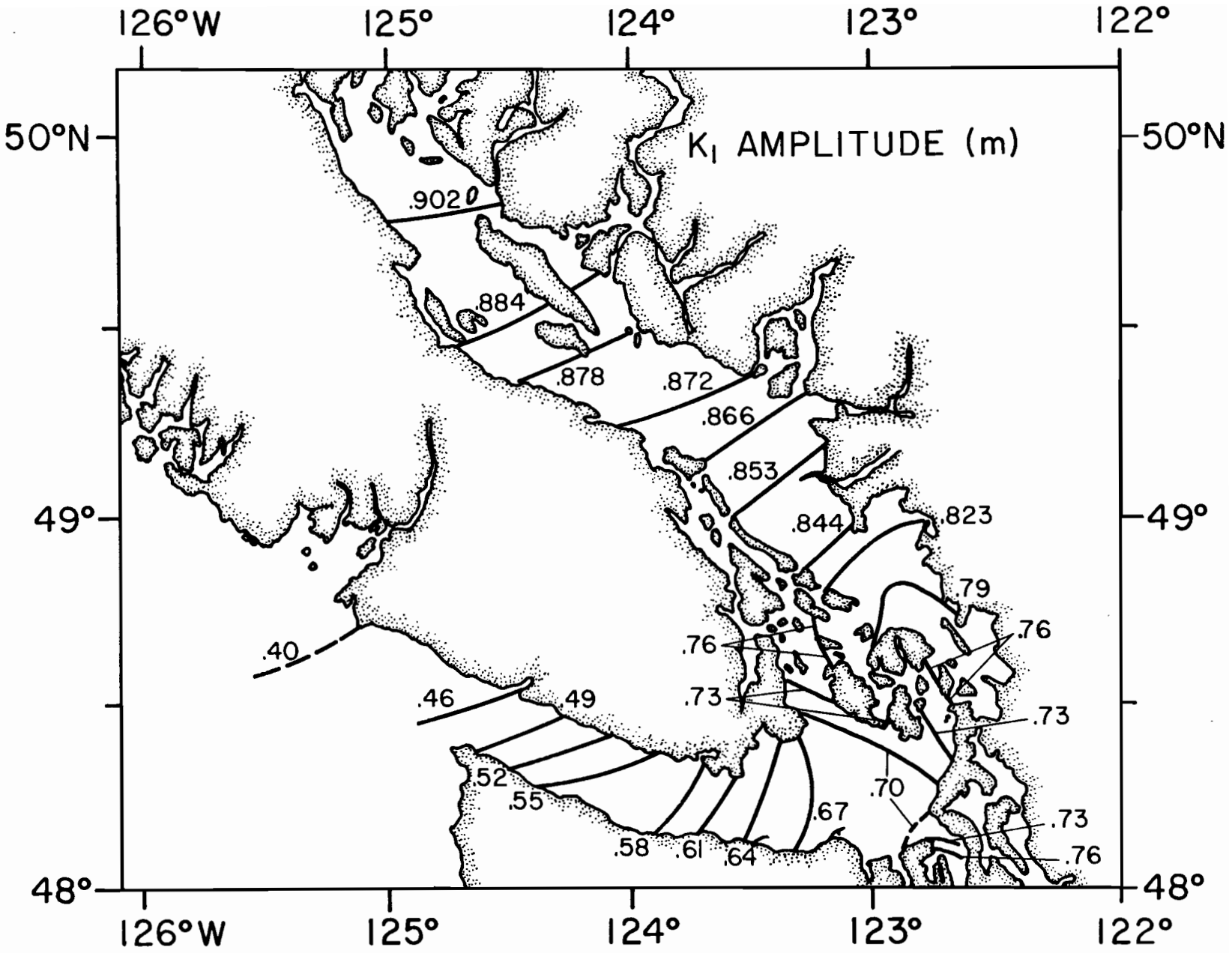

Figure 6. Empirical co-amplitude lines of the K_1 tide in the Straits of Juan de Fuca-Georgia based on a dense net of coastal stations. Dashed lines indicate uncertainty in position. The numbers are amplitudes in meters. Modified from Parker (1977a).

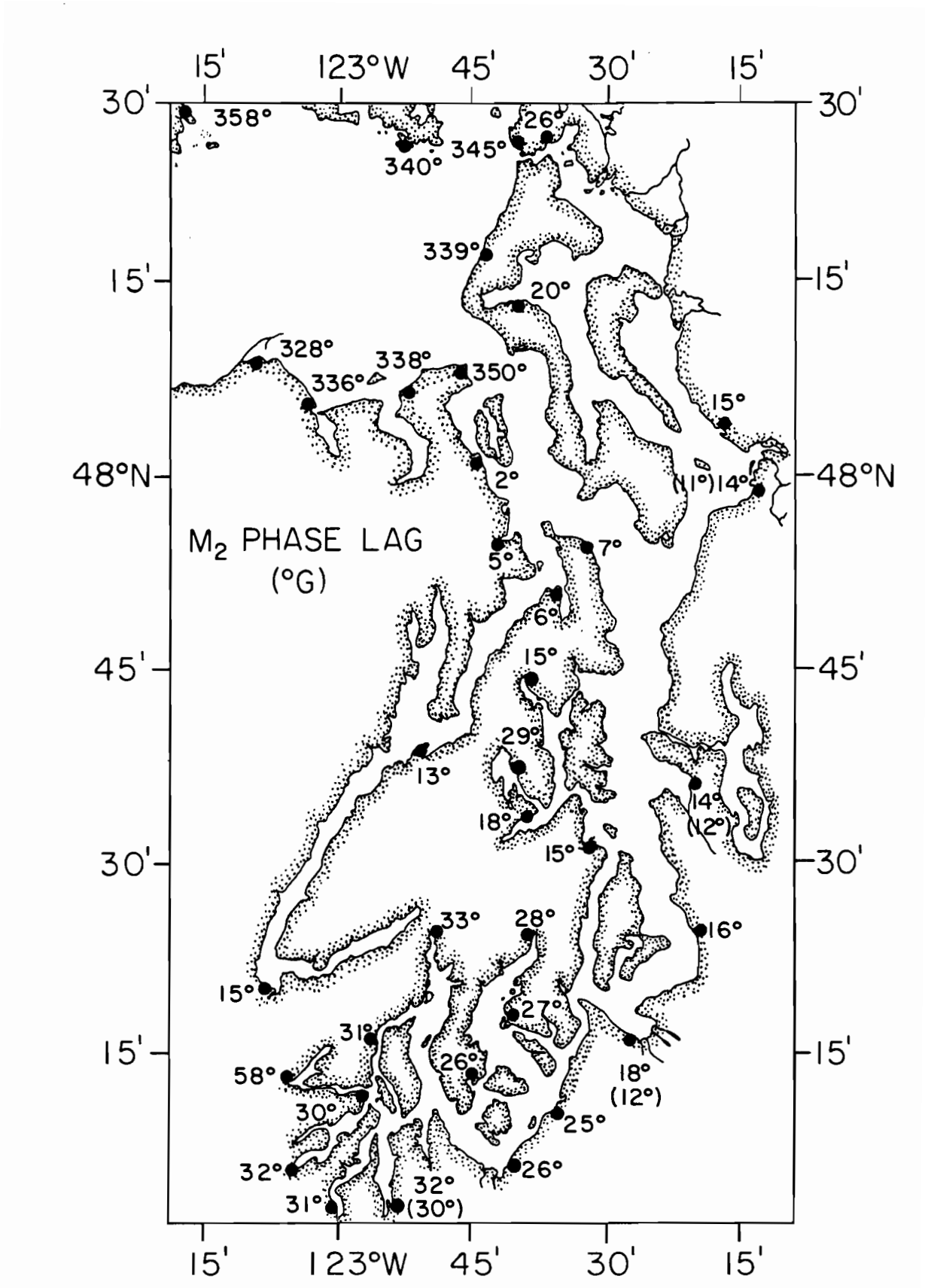

Figure 7. Distribution in Puget Sound of M_2 phase lag in degrees relative to Greenwich transit. From harmonic analyses by the United States Coast and Geodetic Survey and the National Survey (obtained from various sources).

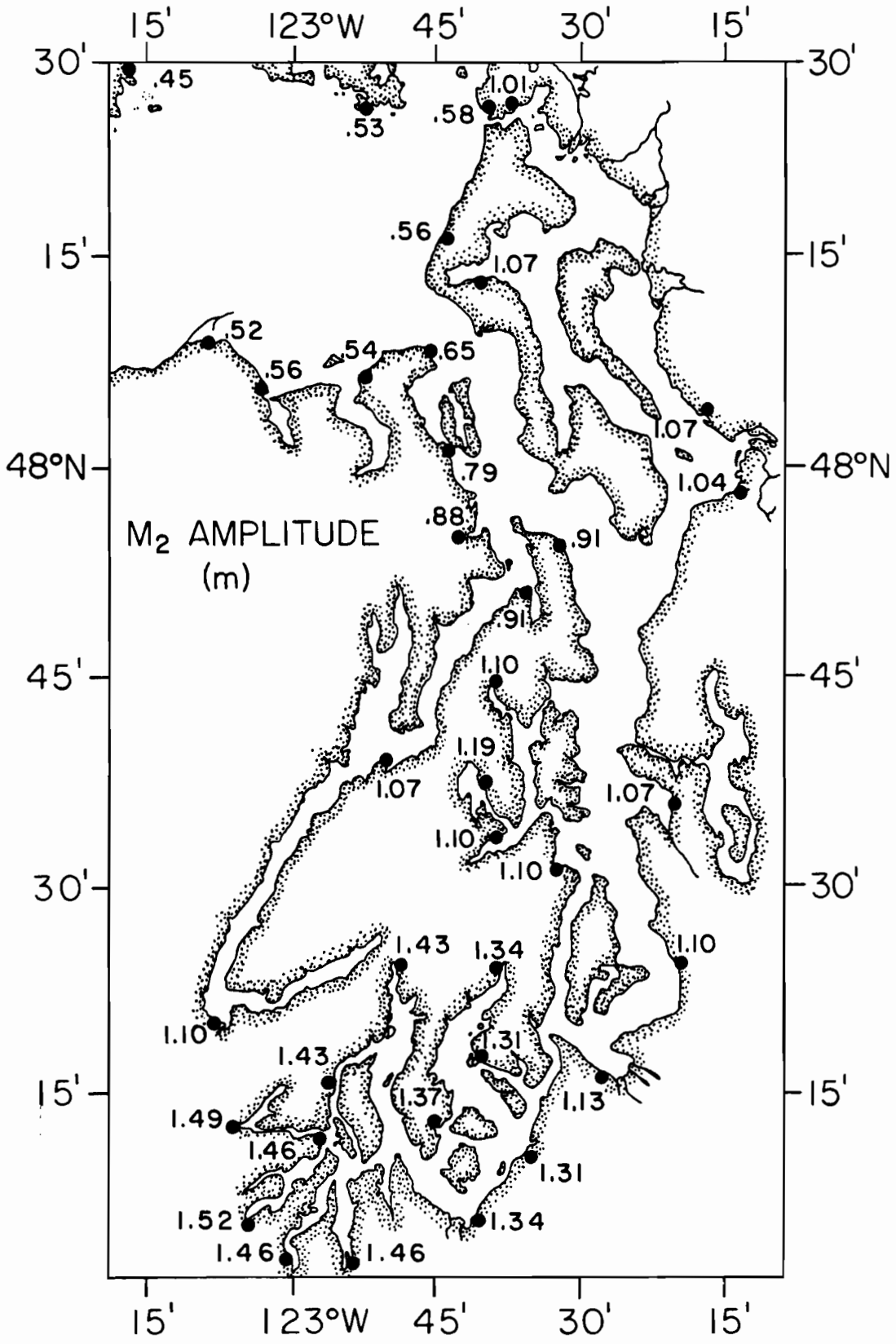

Figure 8. Distribution in Puget Sound of M_2 amplitude in meters. Sources same as Figure 7.

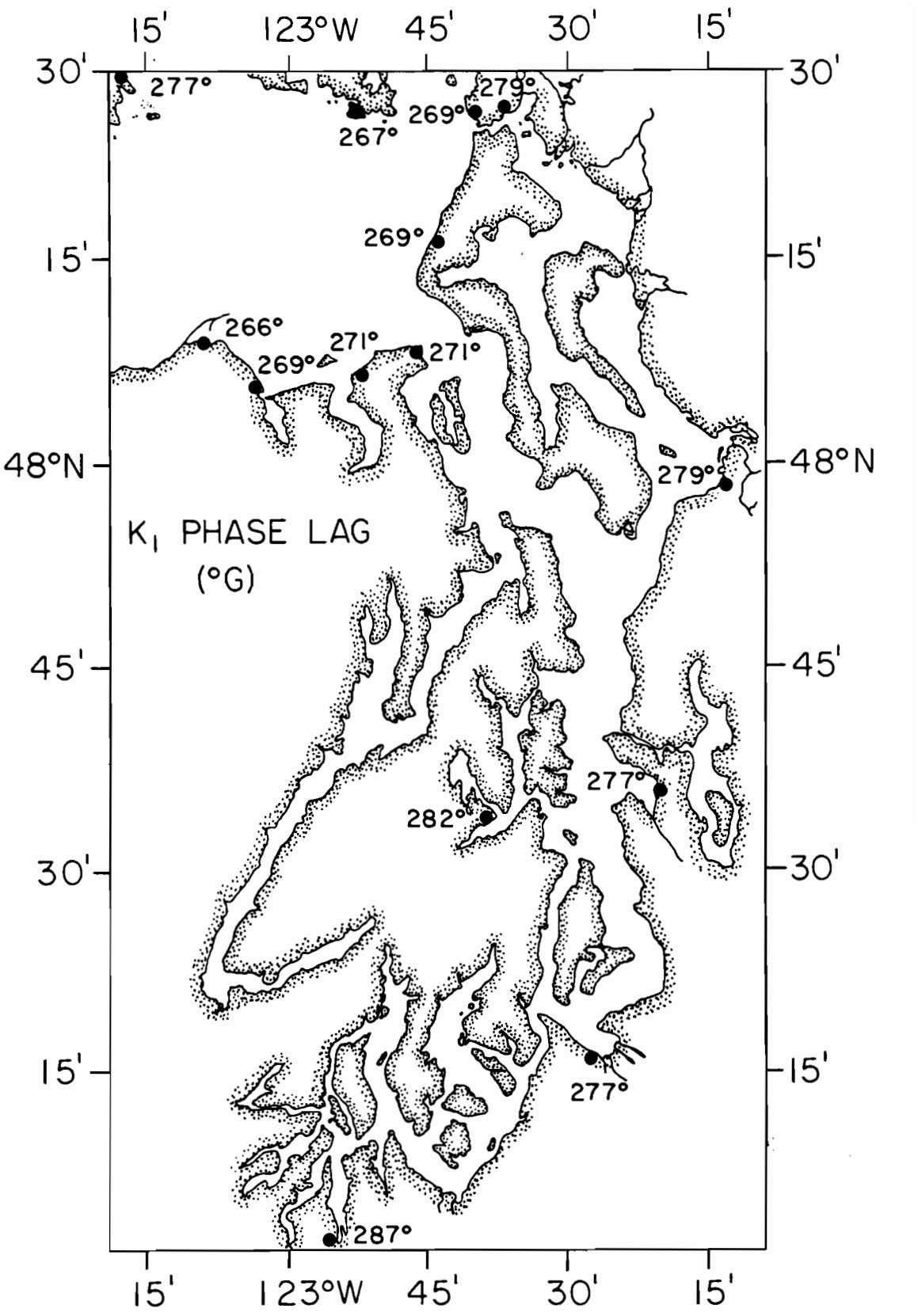

Figure 9. Distribution in Puget Sound of K_1 phase lag in degrees relative to Greenwich transit. Sources same as Figure 7.

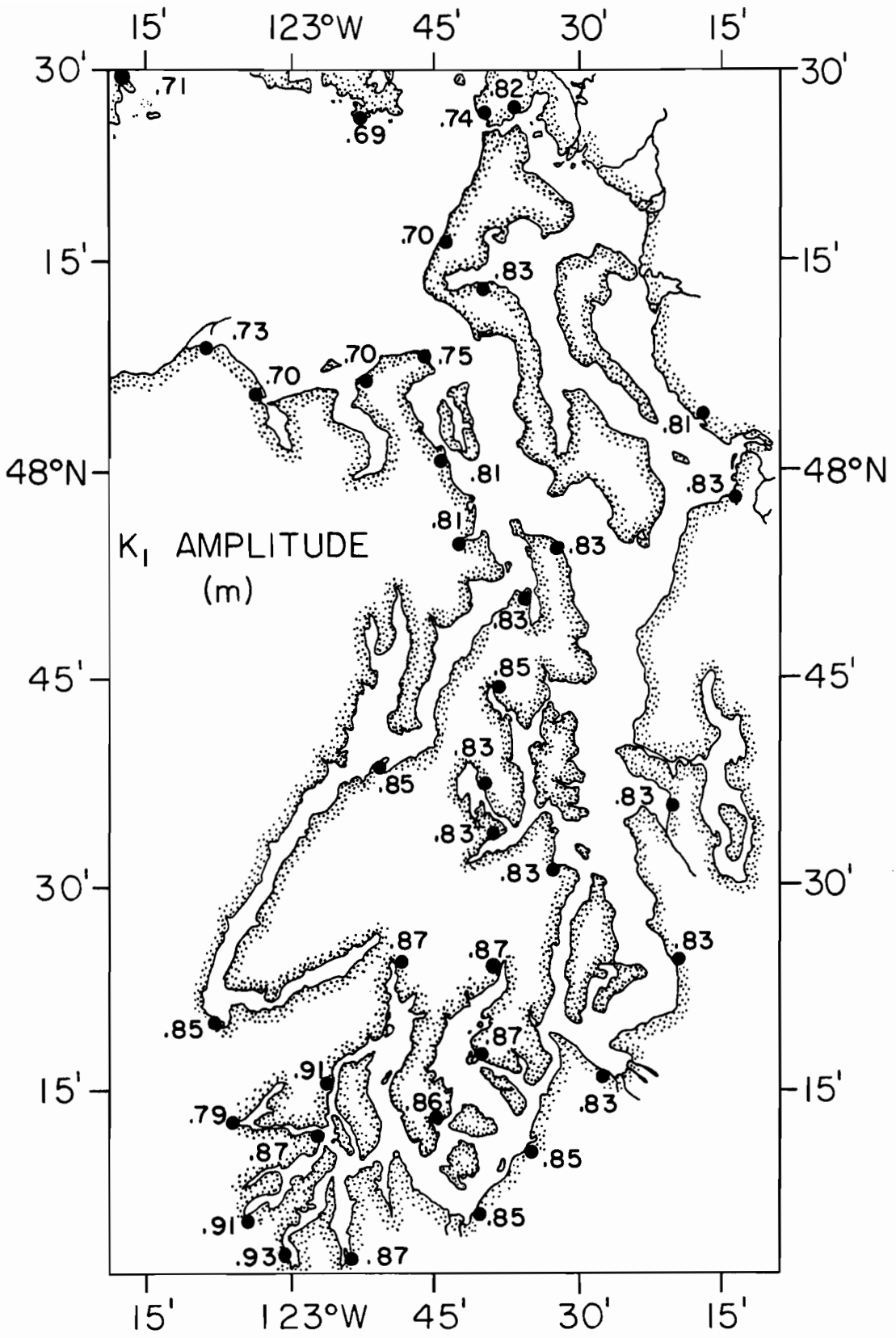

Figure 10. Distribution in Puget Sound of K_1 amplitude in meters. Sources same as Figure 7.

appear to be identified. The tidal distributions in the Straits of Juan de Fuca - Georgia and Puget Sound indicate that the tides are long waves propagating in from the Pacific Ocean and forming standing wave patterns through the combination of incident and reflected waves (Harris 1904, Bauer 1928, Redfield 1950, Rattray in Department of Oceanography, University of Washington 1954, Parker 1980).

The large areas of relatively constant phase and large amplitude are found near reflecting boundaries. These areas include the northern reaches of the Strait of Georgia (Figs. 3 - 6), Southern Basin of Puget Sound (Figs. 7 - 10), Whidbey Basin and Hood Canal. Similar regions in the eastern Strait of Juan de Fuca and the Main Basin of Puget Sound indicate that partial reflection is occurring at intermediate locations along the main channels. The minimum in the M_2 amplitude (Fig. 4) in the eastern Strait of Juan de Fuca is a node formed by the destructive interference of incident and reflected waves. It is located about 1/4 wavelength from the primary reflecting boundary at the northern end of the Strait of Georgia. Because the system is shorter than 1/4 wavelength for the K_1 tide, there is no K_1 node and the K_1 tide therefore increases continuously in amplitude (Fig. 6) from the entrance.

The increase in phase lag with distance into the system is due to frictional dissipation and wave scattering. A bulk estimate (Redfield 1950) of the dissipation can be obtained by fitting the distribution of M_2 and K_1 tides to frictionally damped waves. The fit shows that the dissipation averaged over the Straits of Juan de Fuca - Georgia is significantly greater than in either Long Island Sound or the Bay of Fundy. Crean (1969) finds that a best fit of a coarsely segmented model to observations requires a bottom drag coefficient in the rugged San Juan Archipelago that is an order of magnitude (0.02 to 0.03) larger than generally accepted values (0.002 to

0.004) for open regions with smooth bottoms. Non-linear interactions between tidal constituents (due to the high dissipation in the San Juan Archipelago) are needed to explain the K_1 amplitude in the Strait of Georgia (Crean 1969): Without the non-linear interactions, the K_1 amplitude in the Strait of Georgia would be ~10 cm too small. By fitting a one-dimensional model to observations, Parker (1980) finds that the M_2 tide looses 17% of its amplitude when propagating through the San Juan Archipelago and looses an additional 18% on reflecting at the northern end of the Strait of Georgia. The M_2 tide also looses continuously 53% of its amplitude per wavelength along its path of propagation due to frictional dissipation and wave-scattering. The K_1 tide suffers comparable losses of amplitude (Parker 1980) in the San Juan Archipelago and northern Strait of Georgia, but its continuous decay is much less (10% per wavelength) because the K_1 currents are much less than the M_2 currents and its wavelength is twice as long.

The Straits of Juan de Fuca - Georgia are wide enough to allow major cross-channel variations in the tides. The minimum in M_2 amplitude (Fig. 4) is located on the northern side of the Strait of Juan de Fuca. Explanations for this (Parker 1977b) rely on the effect of the earth's rotation and the influence of Puget Sound: Let us assume that the incident and reflected M_2 waves are damped Kelvin waves with higher amplitude on the right side of the channel, looking in the direction of propagation. At a given cross-section, the amplitude of the reflected wave is smaller than that of the incident wave because of the reflected wave has been attenuated over the path from the cross-section to the reflecting boundary (primarily the northern end of the Strait of Georgia) and back again. As observed the largest M_2 amplitudes should then be along the southern shore of the Strait of Juan de Fuca. The minimum M_2 amplitude is on the northern shore because of sufficient dissipation (Parker 1977b) while the relatively large M_2

amplitudes near the northern end of Admiralty Inlet are due to the co-oscillation with Puget Sound. Harris (1904) associates the influence of the earth's rotation with the crowding of cophase lines on the northern side of the Strait of Juan de Fuca and their spreading on the southern side.

In Admiralty Inlet and The Narrows the large changes of M_2 phase (Fig. 11) are caused by frictional dissipation (Rattray in Department of Oceanography, University of Washington 1954). Friction is also responsible for the large M_2 phase change along the shallow Hammersley Inlet (between Shelton and Arcadia) off the Southern Basin. The change in M_2 amplitude (Fig. 11) between Seattle and the southern end of Admiralty Inlet is probably due to the influence of the Whidbey Basin which increases the effective length of the Main Basin as seen by the tides (Rattray in Department of Oceanography, Univeristy of Washington 1954). The channels and basins of Puget Sound are too narrow to allow large cross-channel variations in the tides.

3. Tidal Currents

Strong tidal currents are common in Puget Sound and the Straits of Juan de Fuca-Georgia; current speeds over 1 m/s can be found in many channels. Weaker tidal currents are prevalent in the deeper reaches while the tidal currents are barely detectable in many side-embayments and blind arms. The transitions in current speeds between these flow regimes are often abrupt and this produces strong tidal fronts. The flow of strong tidal currents past points of land generates eddies which wander through the system. These secondary features associated with the tidal currents are discussed in the next section. In the present section, we shall smooth over secondary

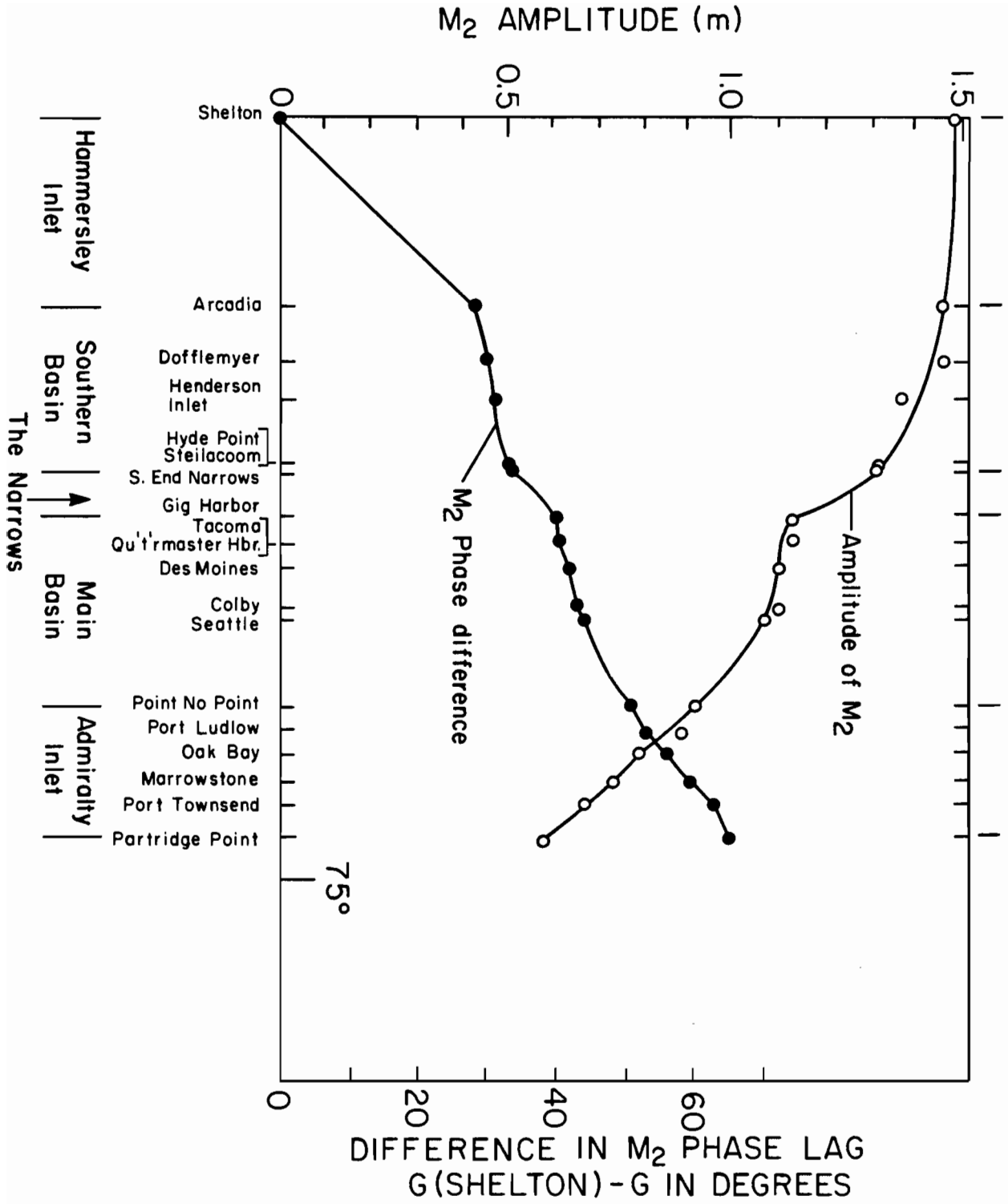

Figure 11. Profiles of M_2 amplitude and M_2 Greenwich phase lag along the main axis of Puget Sound, plotted against the phase of a progressive M_2 wave emanating from Shelton at one head of the Southern Basin in a manner consistent with Redfield's theory (1950) of tides in long embayments. After Rattray in Department of Oceanography, University of Washington (1954).

features and focus on the general characteristics of the tidal currents in the region.

3.1 Geographical Distributions of Tidal Currents

In general, tidal currents of the region vary with depth as well as location. As we shall see, current speeds decrease with depth due to bottom drag and the directions of the currents are relatively independent of depth; coupling to internal waves may also influence the vertical structure of the tidal currents. Each tidal constituent forms a pattern of tidal ellipses; shown in Figures 12 and 13 are the near-surface tidal ellipses for the strongest current constituent M_2. Like the other constituents (Table 4), the M_2 ellipses are narrow and aligned with either the local direction of the channel or a nearby shoreline. The motion is rectilinear in many locations, but broad ellipses do occur (Figs. 12 and 13) where several channels meet.

Strong tidal currents (Fig. 13 and Table 4) occur in Admiralty Inlet and The Narrows. The strongest currents (>4 m/s) in the region flow through Deception Pass in response to large differences in tidal heights (primarily semidiurnal) between the eastern Strait of Juan de Fuca and northern end of the Whidbey Basin. Weak tidal currents prevail in the parts of the Whidbey Basin and Hood Canal that are away from their entrances. Although the Southern Basin occupies one head of the Puget Sound system, strong tidal currents (Fig. 13) occur in all the narrow channels connecting its network of sub-basins. The Strait of Juan de Fuca (Fig. 12 and Table 4) is swept by strong tidal currents. Particularly intense tidal currents (Fig. 12) occur in the straits and channels through the San Juan Archipelago because of the strong co-oscillation between the Straits of Juan de Fuca and Georgia.

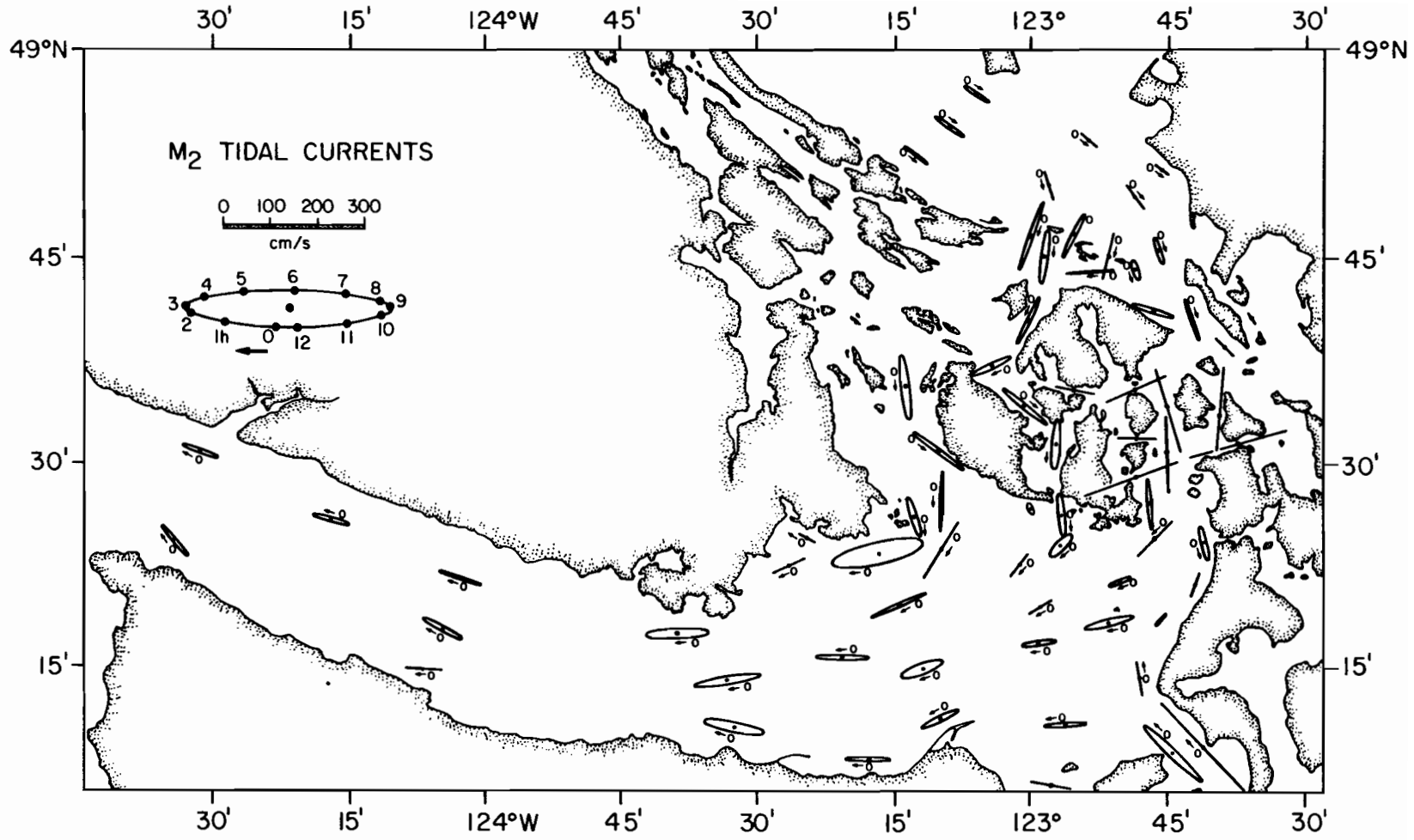

Figure 12. Near-surface M_2 tidal current ellipses observed in the Strait of Juan de Fuca and the southern Strait of Georgia. The M_2 current velocity is a vector extending from the center of a given ellipse to the ellipse itself. The position at Greenwich transit of the velocity vector is indicated by the zero. As time progresses the tip of the vector travels around the ellipse in the direction shown by the arrow. The ellipses were obtained by harmonic analyses of 15- or 29-day series of observations. After Parker (1977a).

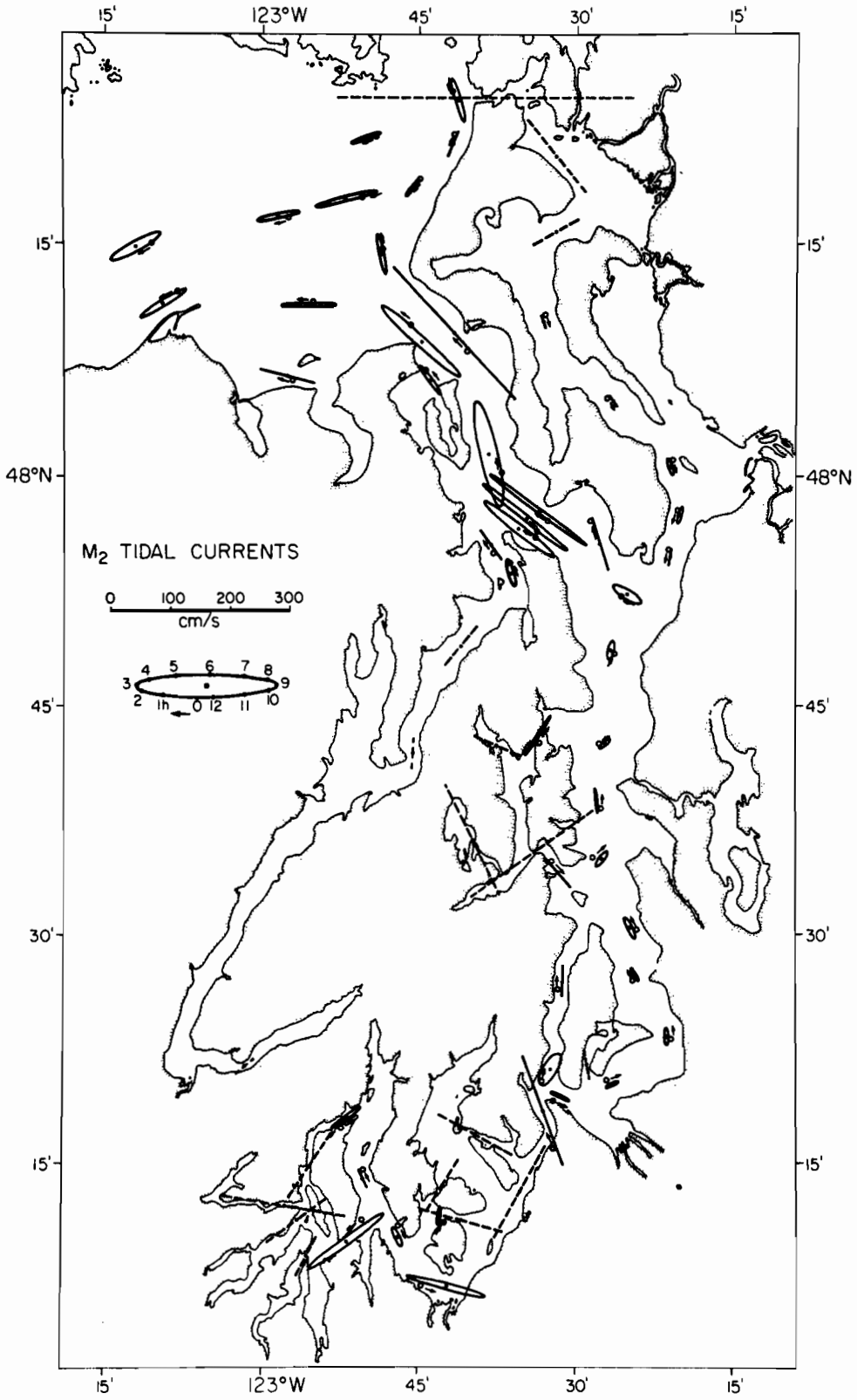

Figure 13. Near-surface M_2 tidal current ellipses observed in Puget Sound. Descriptions of symbols same as Fig. 12. The ellipses were obtained from several sources: 29-day analyses (Table 4) of observations by Cannon et al. (1979), ellipses supplied by Parker (private communication) obtained from a recent observation program by the National Ocean Survey, ellipses from Parker (1977a) and estimates (dashed lines) from the National Ocean Survey Tide Table (1977).

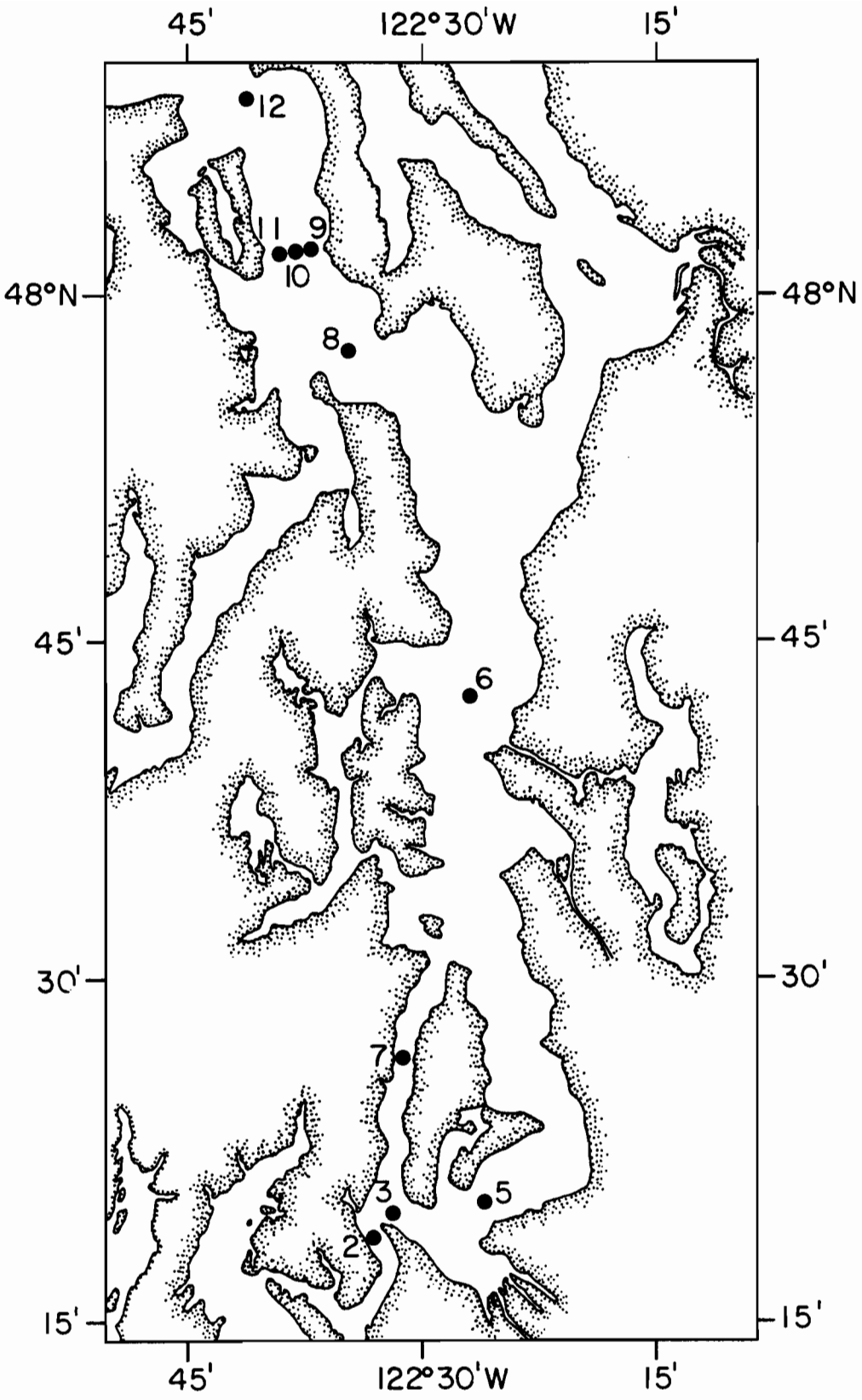

Figure 14. Locations of MESA current stations (Tables 4 and 5) in Puget Sound. After Cannon et al. (1979).

Table 4. Current harmonic constants at selected stations (see Figs. 1 and 14 and Table 5) computed by 29-day harmonic analyses of current observations.

Station	O_1 Amplitude major (cm/s)	O_1 Amplitude minor (cm/s)	O_1 Flood lag G°	O_1 Flood dir T°	O_1 Rot.	K_1 Amplitude major (cm/s)	K_1 Amplitude minor (cm/s)	K_1 Flood lag G°	K_1 Flood dir. T°	K_1 Rot.	N_2 Amplitude major (cm/s)	N_2 Amplitude minor (cm/s)	N_2 Flood lag G°	N_2 Flood dir. T°	N_2 Rot.	M_2 Amplitude major (cm/s)	M_2 Amplitude minor (cm/s)	M_2 Flood lag G°	M_2 Flood dir. T°	M_2 Rot.	S_2 Amplitude major (cm/s)	S_2 Amplitude minor (cm/s)	S_2 Flood lag G°	S_2 Flood dir. T°	S_2 Rot.
ST-1[1]	23.0	5.5	200°	93°	C	38.6	2.4	206°	98°	C	16.1	1.5	253°	126°	CC	58.9	4.0	305°	106°	C	15.6	1.6	310°	118°	CC
25[2]	22.7	4.8	158°	18°	CC	38.8	7.1	196°	7°	CC	21.1	3.6	271°	9°	C	67.0	2.7	299°	0°	CC	16.6	2.3	321°	1°	CC
MESA 12[3]	21.4	0.5	184°	144°	CC	34.5	4.7	200°	134°	C	20.5	2.6	272°	132°	C	89.7	7.5	294°	135°	C	25.2	1.2	328°	131°	CC
MESA 11	13.9	1.8	155°	186°	C	28.4	4.2	173°	174°	C	17.0	1.0	257°	171°	C	87.5	3.2	280°	173°	C	19.5	1.1	302°	169°	C
MESA 10	24.5	6.6	171°	163°	CC	45.6	6.6	204°	164°	CC	21.3	4.1	268°	175°	CC	101.8	13.0	298°	170°	CC	28.7	4.7	325°	172°	CC
MESA 9	23.1	3.7	158°	182°	CC	41.6	2.1	190°	178°	CC	22.6	1.9	257°	175°	C	102.4	5.7	286°	172°	C	27.8	1.8	308°	174°	C
MESA 8	19.3	0.7	162°	140°	CC	39.0	2.1	194°	132°	CC	18.3	1.5	270°	132°	C	96.4	1.8	298°	130°	C	25.0	1.2	324°	134°	C
MESA 6	2.5	0.1	170°	196°	C	7.5	0.6	192°	204°	C	2.6	0.9	269°	198°	CC	14.9	0.6	297°	200°	CC	3.4	0.8	317°	212°	CC
MESA 7	3.4	0.1	251°	170°	C	10.7	0.3	235°	174°	C	5.8	0.5	292°	183°	CC	27.6	0.6	314°	182°	C	7.9	0.4	349°	183°	C
MESA 5	3.6	0.5	160°	219°	C	5.4	0.4	194°	224°	C	2.5	1.1	278°	236°	C	12.9	0.7	290°	243°	C	3.2	0.5	311°	242°	C
MESA 3	9.0	0.8	129°	305°	CC	11.9	1.8	151°	304°	CC	4.6	0.0	251°	289°	CC	28.9	0.9	276°	295°	CC	7.0	1.1	314°	289°	CC
MESA 2	21.7	0.1	136°	155°	C	29.7	0.2	170°	154°	CC	15.3	0.5	263°	152°	C	81.9	0.9	289°	152°	C	19.1	0.2	321°	153°	C

C = clockwise, cc = counterclockwise

[1] from Holbrook et al. (1980)
[2] from Parker (1977a)
[3] for this station and those below: from harmonic analyses by the authors of observations by Cannon et al. (1979).

Table 5. Tidal characteristics and amplitude ratios for the major components of tidal current constituents at selected stations (see Figs. 1 and 14). Values are derived from current harmonic constants in Table 4.

Station	Location latitude / longitude	Depth meter (m)	Depth bottom (m)	Type of tide $\frac{K_1+O_1}{M_2+S_2}$	Sequence of tide $M_2^o-K_1^o-O_1^o$	Major axis current ratios $\frac{O_1}{K_1}$	$\frac{N_2}{M_2}$	$\frac{S_2}{M_2}$	Intervals Luni-tidal (h)	Phase Age (h)	Parallax Age (h)	Diurnal Age (h)
ST-1	48° 14.4N 123° 40.8W	10	170	0.83	259°	0.60	0.27	0.26	10.5	4.9	95.5	5.5
25	48° 27.1N 123° 09.4W	21	132	0.74	305°	0.59	0.31	0.25	10.3	21.6	51.4	34.6
MESA 12	48° 08.7N 122° 41.9W	89	10	0.49	270°	0.62	0.23	0.28	10.1	33.5	40.4	14.6
MESA 11	48° 01.6N 122° 38.9W	51	60	0.40	312°	0.49	0.19	0.22	9.7	21.6	42.3	16.4
MESA 10	48° 01.7N 122° 38.0W	14	108	0.54	283°	0.54	0.21	0.28	10.3	26.6	55.1	30.1
MESA 9	48° 01.8N 122° 37.2W	16	112	0.50	298°	0.56	0.22	0.27	9.9	21.6	53.3	29.2
MESA 8	47° 57.5N 122° 34.5W	15	109	0.48	302°	0.49	0.19	0.26	10.3	25.6	51.4	29.2
MESA 6	47° 42.3N 122° 26.6W	20	200	0.55	295°	0.33	0.17	0.23	10.2	19.7	51.4	20.0
MESA 7	47° 26.5N 122° 31.4W	15	115	0.40	188°	0.32	0.21	0.29	10.8	34.4	40.4	-14.6
MESA 5	47° 20.0N 122° 26.1W	26	181	0.56	296°	0.67	0.19	0.25	10.0	20.7	22.0	31.0
MESA 3	47° 19.4N 122° 31.8W	19	102	0.58	356°	0.76	0.16	0.24	9.5	37.4	45.9	20.0
MESA 2	47° 18.4N 122° 33.4W	43	73	0.51	343°	0.73	0.19	0.23	10.0	31.5	47.8	31.0

3.2 Vertical Dependence of Tidal Currents

How the tidal currents in Puget Sound (Fig. 14) vary with depth depends on the speed of the currents and the total depth. In the high-speed regimes of Admiralty Inlet (Stas. MESA 8 and 10, Fig. 14) observed tidal currents (Fig. 15) decrease rapidly from the surface with strong shear throughout the water column. There is also a hint of strong shear from the near-bottom observations in The Narrows (Sta. MESA 2). The large shear over the water column shows that there is strong turbulence throughout the water column and that strong frictional dissipation is occuring. In the Main Basin (Fig. 15) the tidal current speeds are much less than in Admiralty Inlet and the shear (though not well-resolved) is confined near the bottom; the tidal current speeds are essentially independent of depth over most of the water column.

The phase lag of the tidal currents should decrease with depth because the slower currents nearer the bottom have less inertia to overcome. This is the case (Fig. 15) in Admiralty Inlet (Stas. MESA 8 and 10), Colvos Passage (Sta. MESA 7) and The Narrows (Sta. MESA 6). The K_1 phase lag at MESA 6 increases with depth while the M_2 phase lag decreases as expected. Presently, the behavior of K_1 phase at Sta. MESA 6 is not understood. The directions of the currents (Fig. 15) are relatively independent of depth and essentially the same for diurnal (K_1) and semidiurnal (M_2) constituents. The exception is again Sta. MESA 6 where the tidal currents veer westward with depth.

Holbrook et al. (1980) observe that the tidal currents in the Strait of Juan de Fuca show significant variation with depth in which the ellipses near the bottom are smaller and broader than those near the surface. This is consistent with the results of a seven-level three dimensional numerical study presently in progress (Crean, private communication). Holbrook et al.

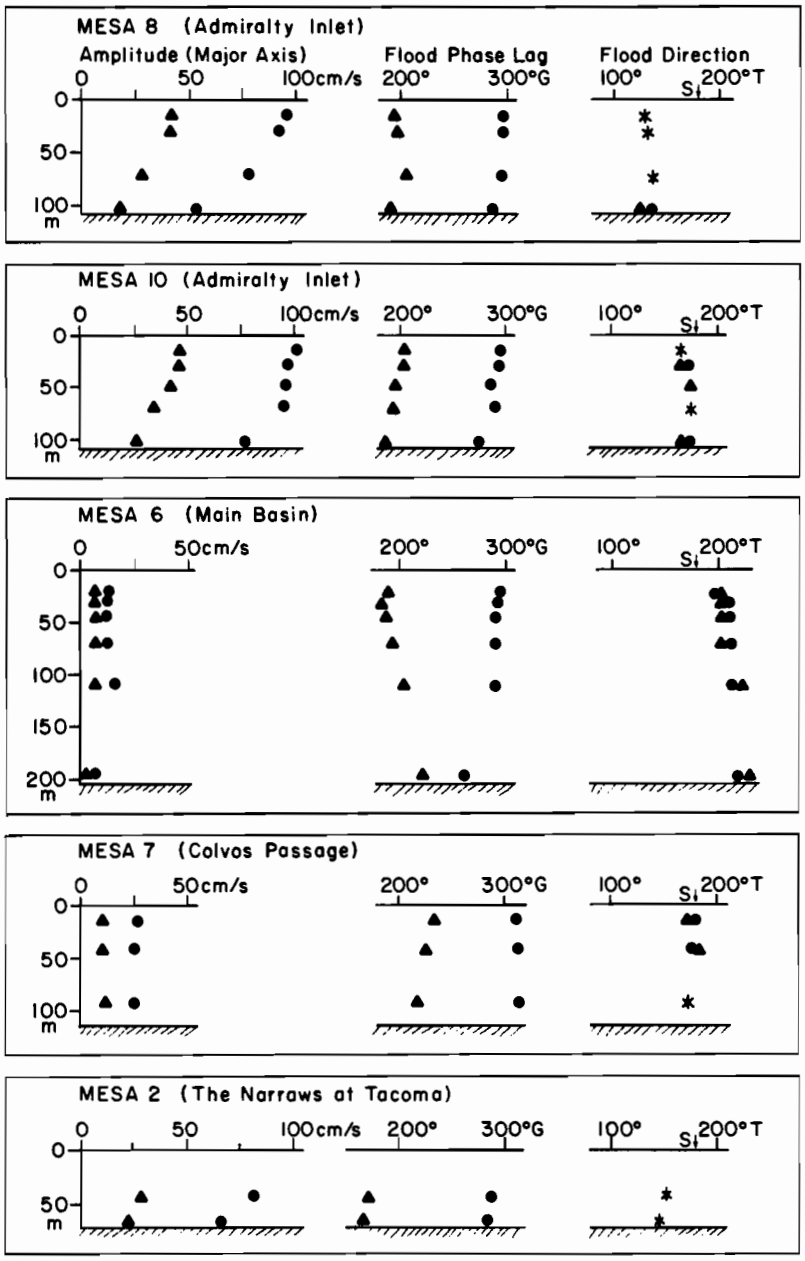

Figure 15. Vertical profiles of the M_2 (solid circles) and K_1 (solid triangles) tidal currents at selected stations (Fig. 14 and Table 4) in Admiralty Inlet and the Main Basin of Puget Sound. (Asterisks indicate equal values for M_2 and K_1). Shown are the amplitudes, Greenwich phase lags and flood (toward the Southern Basin) direction. Values are from 29-day harmonic analyses of observations by Cannon et al. (1979).

(1980) also find seasonal variations and large irregularities in the cross-channel currents near the surface that are due probably to the internal seiching discussed by Crean and Miyake (1976) and Crean (1978). There is also significant vertical shear in the tidal currents near the surface (Holbrook and Frisch 1981). The reasons for this shear are not known at present.

3.3 Patterns of the Tidal Current and Excursion Curves

Like the tides (Fig. 2), the tidal currents (Fig. 16) of the region contain important contributions from both diurnal and semidiurnal constituents. However, the patterns of the tidal current curves differ markedly from those of the tides. The tidal currents (Table 5) are more semidiurnal (type ~0.5). In Puget Sound, the sequence (M_2°-K_1°-O_1°) of the tidal currents (Table 5) vary from about 280° in Admiralty Inlet to 340° in The Narrows. Hence, in Admiralty Inlet there often are major diurnal inequalities in both flood and ebb currents while in The Narrows there often is a major inequality in the flood currents with the ebb-currents of nearly equal strength.

For a pure standing wave the tidal current should lead the tide by 90°; the lead is 0° for a purely progressive wave. The M_2 tidal current at Sta. MESA 6 (Table 4) off Seattle leads the tide (Table 2) at Seattle by 75°; the K_1 lead is 86°. Hence, the phase relationship between the tides and tidal currents near Seattle shows that the tidal motions are due to standing waves with some progression.

Besides the tides and tidal currents, a third kind of tidal motion is the tidal excursion (Table 6). It is the apparent horizontal displacement due to the tidal currents and is the integral over time of the tidal current

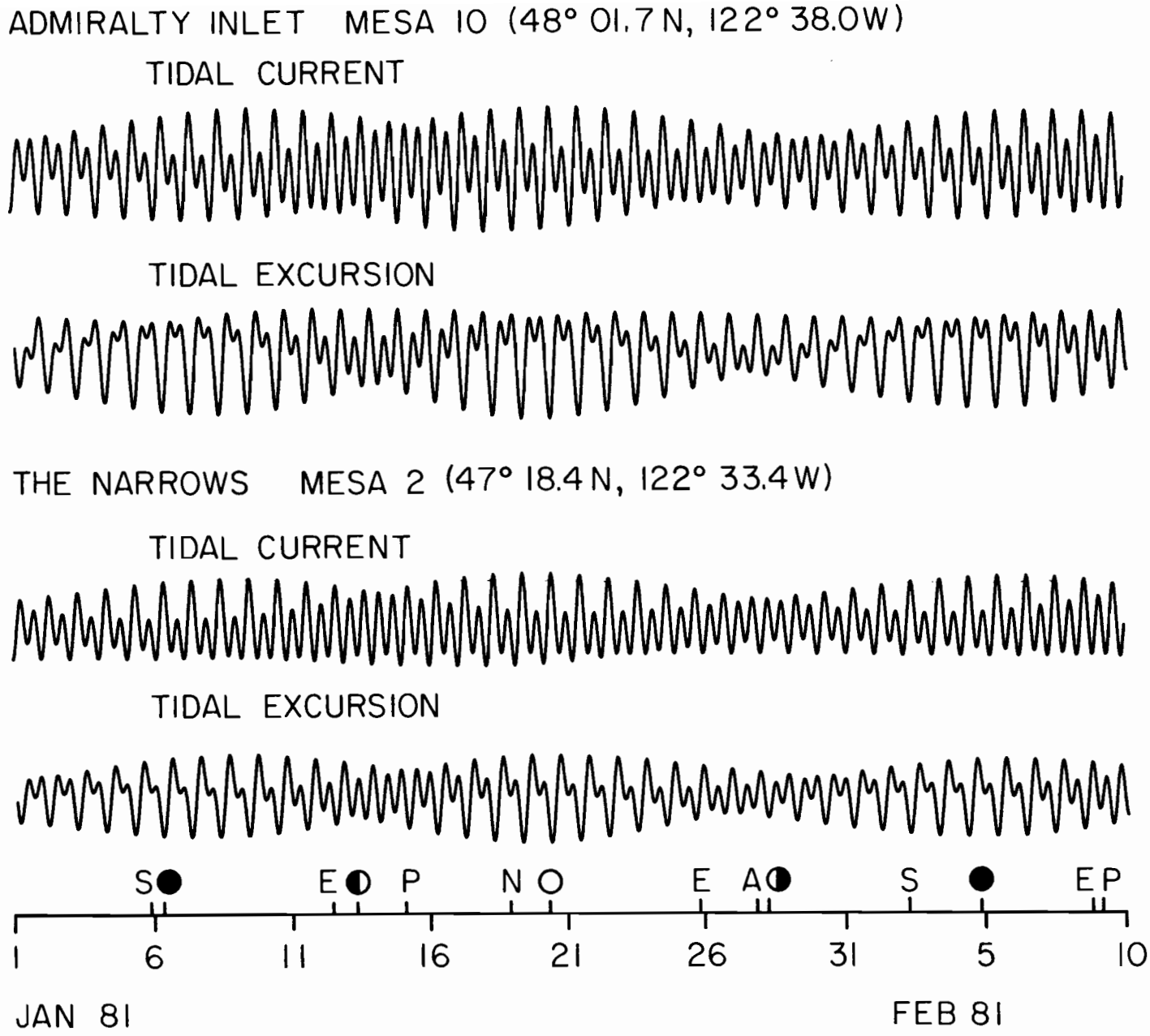

Figure 16. Predicted tidal currents (major component) and excursions at MESA 10 in Admiralty Inlet and MESA 2 in The Narrows (Fig. 14) based on the eight largest constituents observed at these stations. The symbols along the time axis are defined in the caption of Figure 2.

at a given location. In Puget Sound, patterns of the tidal excursions (Fig. 16) resemble closely those of the tides (Fig. 2). This should be the case because both are time-integrals of the tidal currents. The diurnal contribution to the tidal excursions are relatively large compared with their contribution to the tidal currents. This is because the diurnal current flows twice as along as the comparable semidiurnal current. For a given tidal constituent, the tidal current (Table 4) leads the tidal excursion (Table 6) by exactly 90° of phase.

4. Tidal Prisms and Transports

For Puget Sound, a convenient estimate of the water exchanged with the Strait of Juan de Fuca is the average tidal prism defined as the volume between mean high water and mean lower low water. An estimate by Rattray (in Department of Oceanography, University of Washington 1954) of this volume (Table 7) amounts to 8.1 km^3 or 4.8% of the total volume (168.7 km^3) of the Sound. Almost all the exchange is through Admiralty Inlet with a small contribution through Deception Pass. The Main Basin has the largest tidal prism (2.4 km^3) within Puget Sound but because of its large total volume (77.0 km^3) its tidal prism is the smallest (3.2%) percentage of its total volume. The largest percentage (10.6%) change in volume occurs in the Southern Basin. The volume (22.7 km^3) of Admiralty Inlet is 3.7 times the total tidal prism of Puget Sound and there is strong mixing in the Inlet. Admiralty Inlet is therefore a major barrier to direct exchange between the Main Basin and the Strait of Juan de Fuca. The tidal excursion along the axis of Admiralty Inlet can be large enough to allow water from the Strait of Juan de Fuca to traverse the entire Inlet and flow into the Main Basin

Table 6. Tidal excursions[1] and their Greenwich lag[2] for selected current stations (see Figs. 1 and 14) in the Puget Sound region. Values are derived from current harmonic constants in Table 5.

	CONSTITUENTS									
	O_1		K_1		N_2		M_2		S_2	
Station	Excur. (km)	Flood lag (G°)	Excur. (km)	Flood lag (G°)	Excur. (km)	Flood lag (G°)	Excur. (km)	Flood lag (G°)	Excur. (km)	Flood lag (G°)
ST-1	6.8	290°	10.6	296°	2.3	343°	8.4	35°	2.1	40°
25	6.7	248°	10.6	286°	3.1	1°	9.5	29°	2.3	51°
MESA 12	6.3	274°	9.5	290°	3.0	2°	12.8	24°	3.5	58°
MESA 11	4.1	245°	7.8	263°	2.5	347°	12.5	10°	2.7	32°
MESA 10	7.2	261°	12.5	294°	3.1	358°	14.5	28°	3.9	55°
MESA 9	6.8	248°	11.4	280°	3.3	347°	14.6	16°	3.8	38°
MESA 8	5.7	252°	10.7	284°	2.7	0°	13.7	28°	3.4	54°
MESA 6	0.7	260°	2.1	282°	0.4	359°	2.1	27°	0.5	47°
MESA 7	1.0	341°	2.9	325°	0.8	22°	3.9	44°	1.1	79°
MESA 5	1.1	250°	1.5	284°	0.4	8°	1.8	20°	0.4	41°
MESA 3	2.7	219°	3.3	241°	0.7	341°	4.1	6°	1.0	44°
MESA 2	6.4	226°	8.1	260°	2.2	353°	11.7	19°	2.6	51°

[1] Total horizontal distance x_0 between successive times of zero current (slack) along the major current axis $x_0 = \frac{2}{\sigma}u_0$ where σ is the frequency (radians/s) and u_0 is the current (cm/s)

[2] Obtained by adding 90° to the Greenwich lag of the component of current along the major axis

Table 7. Tidal prism (volume between mean high water and mean lower low water) of Puget Sound. Estimates by Rattray in the Department of Oceanography, University of Washington (1954).

Basin	Total Volume[1] (km^3)	Tidal Prism (km^3)	Percentage (%)
Admiralty Inlet	21.7	1.00	4.6
Main Basin	77.0	2.44	3.2
Southern Basin	15.9	1.69	10.6
Hood Canal	25.0	1.14	4.6
Whidbey Basin	29.1	1.83	6.3
Puget Sound (total)	168.7	8.08	4.8

[1] Volume below mean high water

during a single tidal cycle. This occurs when the tidal ranges (>3.5 m at Seattle) are large (Farmer and Rattray 1963). The character of water entering the Main Basin from the Strait of Juan de Fuca must depend in detail on complex processes at work in Admiralty Inlet.

Estimates (Fig. 17) of M_2 transport by Parker (1977a) show that of the 21.3 km^3 entering the eastern Strait of Juan de Fuca from the western Strait, 76% is compensated for by M_2 transport into the passages leading to the Strait of Georgia. Most of this transport (11.0 km^3) flows through Haro Strait with a significant contribution (4.2 km^3) through Rosario Strait. The remaining 24% enters the Puget Sound system through Admiralty Inlet. A comparison of Fig. 17 and Table 7 reveals that the M_2 transport (5.1 km^3) into Puget Sound amounts to 63% of the total tidal prism (8.1 km^3) in the Sound. The relative proportion of M_2 transport between the Strait of Georgia and Puget Sound indicates that the Strait of Georgia dominates the co-oscillation with the Strait of Juan de Fuca but that Puget Sound makes an important contribution to the tidal dynamics of the region.

5. Small-Scale Tidal Features

5.1 Tidal Eddies

The tidal currents in Puget Sound and the Straits of Juan de Fuca-Georgia generate numerous eddies. As shown by the hydraulic model of Puget Sound (Farmer and Rattray 1963, McGary and Lincoln 1977) and the Tidal Current Charts published by the United States Coast and Geodetic Survey (1961), these eddies form nearshore and over shoals.

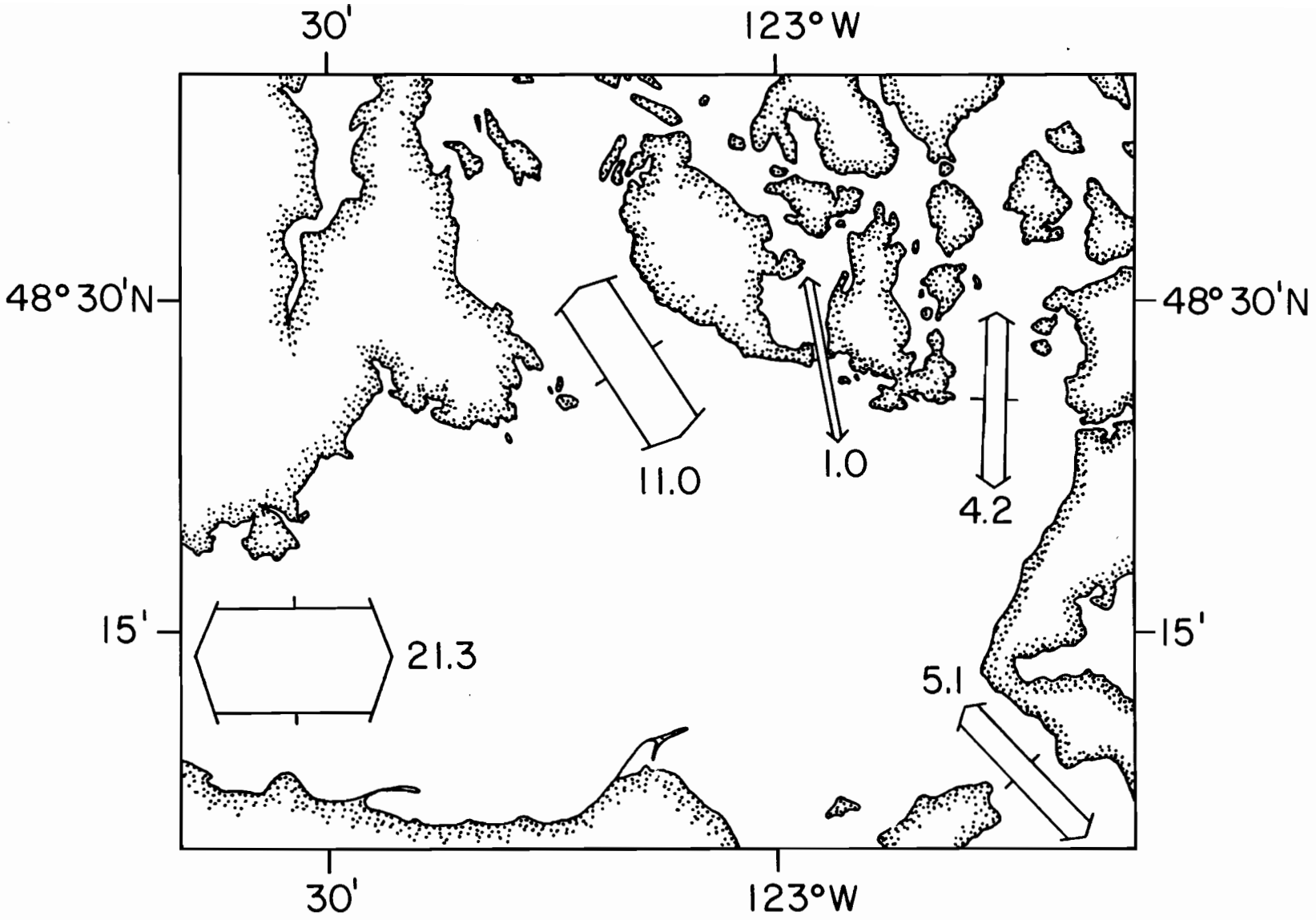

Figure 17. M_2 transports (km^3) across sections leading to the eastern Strait of Juan de Fuca defined as the water transported across a given section during the one flood interval of the M_2 tidal cycle. The tidal prism in the eastern Strait of Juan de Fuca is assumed to be negligible. After Parker (1977a).

Radar observations (Frisch and Holbrook 1980, Frisch 1980) verified by current observations show that the eastern Strait of Juan de Fuca is covered by tidal eddies and fronts. Numerical studies by Crean (1978) indicate that many eddies have current speeds of 50-100 cm/s and produce small-scale fluctuations in sea level of 10-20 cm throughout the eastern Strait. One of the largest and strongest eddies forms at the southern end of Vancouver Island between Race Rocks and Victoria.

In a cove in Hood Canal, Larsen (1976) and Shi (1978) have observed the following sequence during the formation of typical nearshore eddies: Just after the tidal current reverses direction, the flow is parallel to the local isobaths of the cove but deviates in direction toward the direction of flow in mid-channel as the current accelerates. At a critical speed, a small barotropic eddy forms behind the upstream promontory, growing in strength as the tidal current accelerates further. After the tidal current reaches its maximum speed and begins to decelerate, the eddy grows spatially[1] to fill the entire cove and produces a strong nearshore counterflow. The eddy leaves the cove when the tidal current reverses again. There is a minimum speed for the formation of nearshore eddies that probably depends in detail on the local bathymetry. Also in Hood Canal, Jamart and Winter (1978) find from numerical experiments that larger eddies form nearshore and expand into the main channel as the tidal current decelerates. Deep embayments can have pairs of tidal eddies - one near the mouth of an embayment and a second near the head. This is the case in Port Angeles Harbor (Ebbesmeyer et al., 1977) on the southern side of the Strait of Juan de Fuca and Elliott Bay (Sillcox et al., 1981) bordering Seattle in Puget Sound.

---

[1] The spatial growth of eddies during deceleration is consistent with the hydraulic model by Sugimoto (1975) of the Nigushima-Nada Sea.

Observations of currents in Admiralty Inlet (Rattray in Department of Oceanography, University of Washington 1954) show that short period (15 to 45 minutes) fluctuations (~5 cm/s) are more intense near the surface than at depth. The periods of these fluctuations are consistent with eddies (~1 km) being advected by the tidal currents (~50 cm/s). If the fluctuations are nearshore eddies that have been advected into mid-channel from shallow water, the eddies may not been able to penetrate as yet to deep water. Perhaps stratification would be important in inhibiting the downward penetration as observed for eddies near Seattle (Ebbesmeyer et al., 1977). Rattray (in Department of Oceanography, University of Washington 1954) also reports that shorter period (~2 minutes) fluctuations (~10 cm/s) are common in The Narrows; such a short period implies a local source.

There are secondary currents which the tidal currents can create as they flow past the entrance to a channel. At the southern end of the Main Basin, Cannon et al. (1979) observed that sufficiently strong currents flowing northward from The Narrows cause a secondary westward current out of Dalco Passage in the opposite direction to the expected eastward ebb current. There is a minimum speed necessary to produce the secondary current. Cannon et al. (1979) explain the secondary current as the response to the Bernoulli set-down of sea level caused by the tidal current flowing out of The Narrows.

5.2 Tidal Fronts

Major tidal fronts are common in the region. They are the surface expression of tidal convergence zones where near-surface water flows downward at much higher speeds than the vertical velocities caused by the rising and falling of the tides. The tidal fronts often occur where strong

tidal currents flow into basins or larger channels. In Puget Sound, strong tidal fronts (U.S. Coast Pilot, British Columbia Pilot, Frisch 1980) occur at the ends of Admiralty Inlet and off Foulweather Bluff within the Inlet. Satellite observations by Sawyer (Cannon, 1978) show that tidal fronts occur frequently in the eastern Strait of Juan de Fuca, especially near Admiralty Inlet and Haro and Rosario Straits, and in the southern Strait of Georgia. During flood currents, a strong convergence (Frisch 1980) at the northern end of Admiralty Inlet is replaced by a strong divergence. Rattray (in Department of Oceanography, University of Washington 1954) reports that sharp fronts often occur along the edges of tidal eddies. Although they play an important role in the circulation of the region, the tidal fronts and convergences of the region have not been studied in detail.

5.3 Internal Waves

The tidal currents of the region are known to generate two kinds of internal waves. The first kind are groups of high-frequency interval waves that form over sills; the second are internal seiches across channels. Gargett (1976) finds that groups of high-frequency internal waves are common in the southern Strait of Georgia. These waves are generated over sills in the San Juan Archipelago and propagate northward in a two-layer system stratified primarily by effluent from the Fraser River. Similar groups occur in Colvos Passage during ebb (northward) currents as seen in data obtained by Larsen et al. (1977). Seimidiurnal seiches with vertical excursions as large as 50 m have been observed (Crean and Miyake, 1976) in the depth of the pycnocline in the Strait of Juan de Fuca. Holbrook et al. (1980) attribute seasonal variations and irregularities in the observed, cross-channel tidal currents to these internal seiches.

The flow of stratified water over sills generates internal waves. Laboratory observations (Long 1955, 1974; Baines 1976) show that the pattern of flow depends on the Froude number (ratio of upstream current speed to the speed of propagation of the internal waves) and the depth of the sill relative to the depth of the adjacent basin. Making rough estimates of these parameters for the sills in Puget Sound, it appears that almost all the sills should have unsteady patterns of internal motion which never settle down to a steady pattern. Only the sill at the entrance to Dabob Bay (Hood Canal) can have a steady pattern. It is interesting that Dabob Bay contains numerous tidal intrusions at mid-depth (Ebbesmeyer et al., 1975). The flow over its sill allows water to enter Dabob Bay without a great deal of mixing.

6. Summary

The tides and tidal currents of the inland waters of Western Washington originate in the Pacific Ocean. They enter mainly through the Strait of Juan de Fuca with a small contribution through Johnstone Strait at the northern end of the Strait of Georgia. Within the inland waters, the tides propagate as long waves which reflect to form a set of nearly standing waves. In each of the major basins there are large areas in which the amplitudes and phases of the tides are relatively constant. The basins are separated by channels in which the amplitudes and phases of the tides change rapidly with distance. These channels have strong tidal currents and dissipate considerable tidal energy.

Both the diurnal and semi-diurnal tides are important in the region. The tides are mixed-semidiurnal in the western Strait of Juan de Fuca, Puget

Sound south of Admiralty Inlet and in the Strait of Georgia. The tides are mixed-diurnal in the eastern Strait of Juan de Fuca and Admiralty Inlet due to the cancellation of incident and reflected semi-diurnal waves.

The phase relationship of the tidal constituents produce nearly equal high waters with large differences in the low waters when the moon is away from the equator. The forthnightly variations in the tides is due mainly to the tropic-equatorial modulation of the diurnal tides with a smaller contribution due to the spring-neap modulation of the semidiurnal tides. The diurnal range (combined diurnal and semidiurnal) is 2.4 m at the western entrance (Neah Bay) to the Strait of Juan de Fuca. It decreases to 1.9 m at the southern end of Vancouver Island (Victoria) and then increases to 4.4 m at the southern end of Puget Sound (Olympia). The phase lags of the tidal constituents increase moving away from the entrance due to tidal dissipation.

There are seasonal variations in the tides. Near the winter and summer solstices, large tidal ranges and inequalities coincide. Near spring and fall equinoxes the larger ranges have small inequalities while the small ranges have large inequalities. In winter the lowest tides are at night but they occur during the day in summer.

Strong tidal currents (>1 m/s) are common in the Strait of Juan de Fuca and many channels connecting basins. Weaker currents occur in the basins and side-embayments. There are large vertical variations in the tidal currents over sills but the tidal currents are relatively independent of depth in deeper water. The tidal currents are generally aligned with the local channel or shoreline except where the interactions of several channels produces broad tidal ellipses. The phase relationships between the tidal current constituents changes somewhat with location. In Admiralty Inlet there are major diurnal inequalities in both the flood and ebb currents. In

The Narrows major diurnal inequalities occur in the flood currents, but the ebb currents are nearly equal in strength.

The tidal excursions due to the tidal currents are relatively large in sill regions where the currents are strong. The shape of the tidal excursions time-series resemble the time-series of the tides because both are time-integrals of the tidal currents. Associated with the tidal excursions is the tidal prism. This is the volume of water exchanged with a region during a tidal cycle. The tidal prism in Puget Sound is 4.8% of the total volume although it is as large as 10.6% for the Southern Basin. Of the M_2 tidal transport entering the eastern Strait of Juan de Fuca, 76% is compensated by transport into the Strait of Georgia while the remaining 24% is compensated by transport into Puget Sound.

The inland waters of Western Washington are full of small-scale tidal features. Numerous tidal eddies form behind promontories when the current is sufficiently strong. The eddies increase in strength but not size during the accelerating phase of the tidal current. After the tidal current has reached its maximum speed and is decelerating, the eddies increase rapidly in size and detach from the shoreline when the current reverses direction. They are then free to roam through the system. Tidal fronts occur frequently at the transitions from channels into basins and down-current of promontories; they are the surface manifestation of convergence zones where surface water may be downwelled to considerable depth.

Two types of internal waves have been observed in the region. Internal seiches occur in the Strait of Juan de Fuca. Propagating groups of high-frequency interval waves are generated by tidal currents flowing over sills. With the exception of the entrance to Dabob Bay, it appears that the internal waves over sills form unsteady patterns which do not settle down to quasi-steady distributions.

The general distribution of tides and tidal currents in the region appears to be well-established, but the details remain to be worked out. Understanding the influences of tidal motions on the region's oceanography will require a better knowledge of the tidal motions than is presently available. Research at the Pacific Marine Environmental Laboratory and Environment Canada is underway to provide a more quantitative description of the tidal dynamics and the effects of tidal motions.

7. Acknowledgments

This work was supported by the Environmental Research Laboratories, National Oceanic and Atmospheric Administration and by the Office of Marine Pollution Assessment under the LRERP/Sec. 202 Program. The authors wish to thank Professor Clifford Barnes for many helpful discussions of tidal motions in the Puget Sound region. They would also like to thank Bruce Parker (NOS) and Pat Crean (Environment Canada) for their help and comments and Ned Cokelet (PMEL) and Robert Stewart (PMEL) for reviewing the manuscript. A number of people at PMEL contributed to this memorandum: They include Phyllis Hutchens and Lai Lu for typing and Joy Register and Gini Curl for drafting. This memorandum represents Contribution No. 1363 from the School of Oceanography, University of Washington.

8. References

Baines, P.G. (1979) Observations of stratified flow over two-dimensional obstacles in fluid of finite depth. Tellus 31: 351-371.

Bauer, H.A. (1928) Tides of the Puget Sound and adjacent inland waters. Master of Science Thesis, University of Washington, Seattle, Washington, 114 pp.

Canada Department of Mines and Resources (1946) British Columbia Pilot Admiralty Inlet and Puget Sound: 41-79. Vol. I, Southern portion of the coast of British Columbia, 4th Ed., Hydrographic and Map Service Surveys and Engineering Branch, Ottawa.

Cannon, G.A., (ed.) (1978) Circulation in the Strait of Juan de Fuca; some recent oceanographic observations. NOAA Technical Report ERL-PMEL 29, 49 pp.

Cannon, G.A., N.P. Laird and T.L. Keefer (1979) Puget Sound Circulation: final report for FY77-78. NOAA Technical Memorandum ERL MESA-40, 55 pp.

Cox, J.M., C.C. Ebbesmeyer, C.A. Coomes, L.R. Hinchey, J.M. Helseth, G.A. Cannon and C.A. Barnes (1981) Index to observations of currents in Puget Sound, Washington, from 1908-1980. NOAA Technical Memorandum OMPA-5, 51 pp.

Crean, P.B. (1969) A one-dimensional hydrodynamical numerical tidal model of the Georgia-Juan de Fuca Strait System. Fisheries Research Board of Canada Technical Report 156, 32 pp.

Crean, P.B. and M. Miyake (1976) STD sections Strait of Juan de Fuca, March-April 1973. Data Report 38 (Provisional) Institute of Oceanography, University of British Columbia.

Crean, P.B. (1978) A numerical model of barotropic mixed tides between Vancouver Island and the mainland and its relation to studies of the estuarine circulation. In: Nihoul, J.C.J. (ed.), Hydrodynamics of Estuaries and Fjords, 283-313, Elsevier, Amsterdam.

Ebbesmeyer, C.C., C.A. Barnes and E.W. Langley (1975) Application of an advective-diffusive equation to a water parcel observed in a fjord. Estuarine and Coastal Marine Science 3: 249-268.

Ebbesmeyer, C.C., J.M. Helseth, C.A. Barnes, J.H. Lincoln and W.P. Bendiner (1977) On nearshore trapping of pollutants by tidal eddies downstream from points in Puget Sound, Washington 134-145. Proceedings of The Use, Study and Management of Puget Sound, University of Washington WSG-WO77-1.

Farmer, H.G. and Rattray, Jr. (1963) A model study of the steady-state salinity distribution in Puget Sound. Department of Oceanography Technical Report 85, University of Washington, 33 pp.

Frisch, S. and J. Holbrook (1980) HF radar measurements of circulation in the eastern Strait of Juan de Fuca (August, 1978). Interagency Energy/ Environment R & D Program Report EPA-600/7-80-096, 266 pp.

Frisch, S. (1980) HF radar measurements of circulation in the eastern Strait of Juan de Fuca near Protection Island (July, 1979). Interagency Energy/Environment R & D Program Report EPA-600/7-80-129, 133 pp.

Gargett, A.E. (1976) Generation of internal waves in the Strait of Georgia, British Columbia. Deep-Sea Research 23: 17-32.

Harris, R.A. (1904) Cotidal lines for the world. In: Manual of Tides - Part IVB. Reports of the U.S. Coast and Geodetic Survey, Appendix 5, 400 pp.

Hicks, S.D. (1973) Trends and variability of yearly mean sea level 1893-1971. NOAA Technical Memorandum NOS 12, 13 pp.

Holbrook, J.R., R.D. Muench, G.G. Kachel and C. Wright (1980) Circulation in the Strait of Juan de Fuca: recent oceanographic observations in the eastern basin. NOAA Technical Report ERL 412-PMEL 33, 42 pp.

Holbrook, J.R. and A.S. Frisch (1981) A comparison of near-surface CODAR and VACM measurements in the Strait of Juan de Fuca, August 1978. Journal of Geophysical Research 86: 10908-10912.

Jamart, B.M. and D.F. Winter (1978) A new approach to the computation of tidal motions in estuaries. In: Nihoul, J.C.J. (ed.) Hydrodynamics of estuaries and fjords: 261-281. Elsevier, Amsterdam.

Larsen, L.H. (1976) Observations of winds and currents in Hood Canal. University of Washington, Department of Oceanography Technical Report 350, 34 pp.

Larsen, L.H., N. Shi and J.G. Dworski (1977) Current meter observations in Colvos Passage: Puget Sound, March 1977. University of Washington, Department of Oceanography Special Report 82, 50 pp.

Long, R.R. (1955) Some aspects of the flow of stratified fluids. III. Continuous density gradients. Tellus 7: 341-357.

Long, R.R. (1974) Some experimental observations of upstream disturbances in a two-fluid system. Tellus 26: 313-317.

Marmer, H.A. (1951) Tidal datum planes. United States Dept. of Commerce, Coast and Geodetic Survey Special Publication 135, 142 pp.

McGary, N., and J.H. Lincoln (1977) Tidal Prints, University of Washington Press, Seattle, 51 pp.

National Ocean Survey (1981) United States Coast Pilot 7, Pacific Coast: California, Oregon, Washington and Hawaii. 17th Ed., United States Department of Commerce, Washington, D.C., 423 pp.

National Ocean Survey (annual after 1971) Tidal tables, West Coast of North and South America including the Hawaiian Islands. United States Department of Commerce.

National Ocean Survey (annual after 1971) Tidal current tables. Pacific Coast of North and South America and Asia. United States Department of Commerce.

Parker, B.B. (1977a) Tidal hydrodynamics in the Strait of Juan de Fuca - Strait of Georgia. NOAA Technical Report NOS 69, 56 pp.

Parker, B.B. (1977b) Tidal hydrodynamics in a long narrow estuary. Transactions American Geophysical Union 58: 404.

Parker, B.B. (1980) The attenuation of tidal waves in a long narrow semi-enclosed basin. Transactions, American Geophysical Union 61: 273.

Redfield, A.C. (1950) The analysis of tidal phenomena in narrow embayments. Papers in Physical Oceanography and Meteorology 11(4), 36 pp. Massachusetts Institute of Technology and Woods Hole Oceanographic Institution.

Shi, N.C. (1978) A study of the nearshore current observations in Hood Canal, Washington. Master of Science Thesis, University of Washington, Seattle, Washington. 96 pp.

Sillcox, R.L., W.R. Geyer and G.A. Cannon (1981) Physical transport processes and circulation in Elliott Bay. NOAA Technical Memorandum OMPA-8, 45 pp.

Sugimoto, L. (1975) Effect of boundary geometries on tidal currents and tidal mixing. Journal of the Oceanographical Society of Japan 31: 1-14.

United States Coast and Geodetic Survey (1961) Tidal currents charts, Puget Sound, northern and southern parts, 2nd Ed., U.S. Dept. of Commerce, Rockville, 12 pp. ea.

University of Washington, Department of Oceanography (1954) Puget Sound and approaches, a literature survey. Vol. 3, Section 10, Physical oceanography: 1-116. Office of Naval Research Contract Nonr 447(00), Task Order 477(06) (Unpublished manuscript).

Waldichuk, M. (1964) Daily and seasonal sea-level oscillations on the Pacific Coast of Canada, Studies in Oceanography, 181-201. K. Yoshida, ed., University of Washington, Seattle, 568 pp.

Zetler, B.D. (1959) Tidal characteristics from harmonic constants. Journal of the Hydraulic Division, Proceedings of the American Society Civil Engineers, HY 12, 77-87.